earth

MDPI

Article

Morphology and Sedimentology of La Maruca/Pinquel Cobble Embayed Beach: Evolution from 1984 to 2024 (Santander, NW Spain)

Jaime Bonachea [1,*] and Germán Flor [2]

[1] Department of Earth Sciences and Condensed Matter Physics, Universidad de Cantabria, Avenue/Los Castros, 48, 39005 Santander, Spain
[2] Department of Geology, Universidad de Oviedo, Street/Jesús Arias de Velasco, s/n, 33005 Oviedo, Spain; gflor@uniovi.es
* Correspondence: jaime.bonachea@unican.es

Abstract

This study investigates the morphodynamic evolution of an embayed cobble beach located on a mesotidal cliff coast in northern Spain. La Maruca/Pinquel beach was selected for its distinctive geomorphological setting, perched on a well-sorted cobble substrate and bordered by a slightly elevated (less than 1 m) wave-cut platform. Firstly, the availability of orthophotos and the achievement of field surveys enabled a detailed topographic mapping of morphological features. Sedimentological analyses based on grain size and clast shape revealed characteristics indicative of prolonged low-energy wave conditions. A permanent sharply crested ridge and ephemeral staggered tidal berms define the morphology of the beach. Additional depositional features such as washovers, tabular structures, and lobes are also well developed. Sediment accumulation is most pronounced in the western sector, where overwash lobes migrate landward. A W-to-E gradient in cobble size and the presence of boulders in the lower foreshore can be observed. Secondly, a morphosedimentary model was developed based on the obtained data to interpret the beach's dynamic behavior under current and projected coastal forcing. Finally, by analyzing orthophotographs spanning a 40-year period (1984–2024), the long-term geomorphological evolution of the beach was documented. The results reveal significant morphological transformations, notably a shoreline retreat of approximately 12 m and a reduction in the cobble-covered surface area, among other findings. Future analyses of sediment transport processes and lithological responses to erosion will be able to offer a deeper understanding of the complex behavior and resilience of pebble beach systems in response to changing environmental conditions.

Keywords: cobble beach; granulometries; clast shapes; trend maps; historical evolution

Academic Editor: Christian Conoscenti

Received: 22 October 2025
Revised: 27 November 2025
Accepted: 9 December 2025
Published: 15 December 2025

Citation: Bonachea, J.; Flor, G. Morphology and Sedimentology of La Maruca/Pinquel Cobble Embayed Beach: Evolution from 1984 to 2024 (Santander, NW Spain). *Earth* **2025**, *6*, 159. https://doi.org/10.3390/earth6040159

1. Introduction

Beaches are depositional environments in continuous change, regardless of their sediment composition. Sediment studies are essential to comprehend the fundamental characteristics and distribution of sedimentary deposits on beaches. The morphology of the beach over time is determined by the characteristics of these sediments, primarily influenced by coastal agents and human activity (predominantly nourishment operations) and their distribution along the beach [1]. The use of aerial images or orthophotos facilitates the analysis of the changes to deposits and the evolution of the beach in current times [2], which can then be used for future coastal planning and managing the coast in future.

Sediments in beaches are characterized by grain size, mineralogical composition, and particle shape [3]. Grain size is a fundamental property in the study of beaches, as it is used to perform a simple first-order classification to define the state of a beach [4,5]. Particle shape analysis is an important physical attribute of the hydrodynamic behavior of particles in a medium of transportation [6,7]. In addition, the spatial distribution of sediments is related to the variability of incident waves [8], tide range [9], and induced currents.

Beaches composed mainly of sand, which attract a significant population that represent an economic resource [10], have traditionally garnered more attention than beaches composed of larger deposits, which are less attractive to tourists. Also, the analysis of sedimentary parameters in pebble/cobble/boulder beaches is more complicated due to the difficulty of walking through such deposits (gravel and larger-sediment beaches are relatively common on rocky coasts around the world) [5,11,12] and because a more labor-intensive approach is needed. This type of beach is more active during stormy periods, with storm surges manifesting themselves in the form of cliff edge erosion; their retreat rates, however, are very slow [13].

In the previous literature, several works have studied the variability of coarse grain size in gravel beaches and the permeability of these sediments under the action of waves [14]; others have analyzed the response to wave reflection and transmission, the wave run-up (i.e., the maximum vertical reach after the wave breaks on the beach) [15,16], the overtopping [17], and other insights. In [18], the author analyzed the sedimentology of the Aramar gravel beach (Luanco, Asturias, Cantabrian Sea), a Sker-type beach [19], and deduced its dynamics in a seasonal cycle that includes beach rotations. The majority of Cantabrian gravel beaches are comparable to the Sker-type, the kind of beach that undergoes significant cyclical changes; however, these beaches have not yet been the subject of detailed study. Two types of beaches can be found in the Cantabrian coast: embayed beaches and pocket beaches [20]. While embayed beaches present clasts or terrigenous materials, mainly produced by cliff erosion, some pocket beaches have been filled with river gravels.

In the present study, the relationship between mean grain size and other graphic textural parameters (size versus roundness, sphericity, and oblate–elongate index) are plotted [6], as these parameters enable the analysis of hydrodynamic conditions, mode of transportation, and deposition of detrital sediments [21]. Clast roundness, flatness, and rate of mechanical destruction depend on wave intensity, initial rock type, and nature of the coast, i.e., whether this is sheltered or exposed [16].

This study aims to analyze La Maruca/Pinquel cobble beach through the following objectives:

- Identification and mapping of the various morphologies present on the beach, along with their spatial and temporal distributions, using high-quality orthophotos;
- Characterization of the granulometric and particle shape parameters across the entire fieldwork;
- Correlation between the granulometric characteristics and the coastal dynamic processes influencing the area;
- Proposal of a projection of the beach's future evolution based on observed trends over the past 40 years, which can be used as a model for managing beaches in other coastal areas.

The results obtained here will be of aid in future development plans for this Atlantic beach and other beaches with similar characteristics.

2. Study Area

La Maruca/Pinquel beach is a "pure" gravel beach, which contains calcareous gravels belonging mainly to the pebble fraction, without sediment inputs or outputs. The beach presents steep and typically concave profiles seaward with increasing slope up the beachface [22], steeper than those in sandy beaches.

La Maruca/Pinquel beach contains coarse fractions of isotropic sandy micritic limestone cobbles, with average sizes greater than the pebble fraction (>60 mm). Most cobbles are subrounded and light gray in tone, representing a typical perched beach (Figure 1C) with no lateral or frontal sediment continuity.

This beach is located in the westernmost part of the coastal cliff section of the municipality of Santander (Cantabria, northern Spain) (Figure 1), which is part of the recently declared UNESCO Global Geopark (UGGp) Costa Quebrada. Its geographical location (43° 28′ 50″ N, 3° 50′ 23″ W) is close to La Maruca estuary, which has been observed to register significant sedimentation rates [23].

From a geological point of view, La Maruca/Pinquel beach is located on the marine limestone complex of the Lower Eocene—within the Basque–Cantabrian Basin in the northern side of the municipality of Santander—a domain that experienced a minor subsidence in the so-called Santander Coastal Block [24]. The beach is installed on the Peña Saría Formation (Ypresian age; 48–54 Ma), with a maximum visible thickness of 150 m and made of generally very sandy limestones that may contain flint. The underlying Estrada Formation consists of limestone with Alveolines and Nummulites [25,26]. The layers dip about 30° to the NW and are intensely jointed with preferential directions NE–SW and NW–SE, creating a polygonal mosaic well represented as wave-cut platforms.

The coastal profile is cut in a NE–SW direction, drawing a gentle arc with its concavity toward the NW. The coast is cliff-lined with escarpments that do not exceed 50 m in height, more abrupt toward the NE.

Figure 1. (**A**) Location of Santander municipality in SW Europe. (**B**) La Maruca/Pinquel cobble beach on the Cantabrian coast. (**C**) Oblique photo of La Maruca/Pinquel cobble beach, developing an upper storm crest and some staggered tide berms, arched in a concave-seaward plane shape [27].

3. Materials and Methods

3.1. Acquisition of Historical Orthophotographs and Geomorphological Mapping

To investigate the evolution of La Maruca/Pinquel beach in recent decades, the existing orthophotographs for the study area were consulted and implemented in the ArcGis Pro Geographic Information System (GIS). These images are freely available from the Government of Cantabria [28] and the National Geographic Institute of the Spanish Government [29]. The images used here correspond to the National Aerial Orthophotography Plan (PNOA) [30] of Spain for the years 1984, 2002, 2007, 2010, 2014, 2017, 2020, 2023, and 2024 (Table 1), in accordance with the European Inspire directive. Flights are generally scheduled during the summer months as, at these latitudes, weather conditions are more favorable then for aerial imaging. Orthophotographs are georeferenced images, so no further processing is required. The resolution of the orthophotos used in the present work ranges from 15 to 25 cm (pixel size).

Table 1. Characteristics of the images used in this study. The connection server for adding the orthophotos to a geographic information system (GIS) is indicated. Geographic information is referred to ETRS89, Zone 30N, Geodetic Reference System.

Flight Date	Resolution (cm)	GSD: Ground Sample Distance (cm)	RMSE: Root Mean Square Error (cm)	Source of the Images
14–15 September 2024	25	25	50	[28,29]
7 August 2023	15	15	30	[28,29]
29 September 2020	15	15	30	[28,29]
3 July 2017	25	No Data	No Data	[28,29]
27 July 2014	25	25	50	[28,29]
5 September 2010	25	50	100	[28,29]
5 September 2007	25	10	20	[28,29]
10 September 2002	25	50	50	[28,29]
November 1984	25	50	100	[29]

It is evident that the optimal scenario would involve the acquisition of high-quality images on an annual basis, thereby enabling the annual observation of changes. However, this is not a feasible option. In the case of satellite images, or even LIDAR, these are also unavailable.

Once the orthophotographs were incorporated into the GIS, the main features and elements observable at this scale were mapped on each image, using always a visible scale of 1/250 to maintain the same observation criteria.

The existence of high-resolution orthophotographs, in conjunction with the researchers' experience in such environments, facilitates the identification of the beach's topography. The topography of the beach could be extracted using numerical or automatic methods. However, it should be noted that high-resolution techniques are not available for the period analyzed in this work.

Due to the resolution and georeferencing of the images, the following geomorphological features could be identified and mapped: coastal paths, cliffs, contour of cobble deposits, crests of the tide and storm berms, ponds, and rocky substrate. It is therefore possible to estimate areas and lengths for different time periods.

Based on the orthophotographs, the field campaign was designed considering the distinctive characteristics of the beach and the expertise of the researchers in this field. As a result, seven representative cross-sectional profiles (I to VII), distant among them and between 15 and 18 m, were proposed on the shoreface, the low-tide depression (due to its rarity), and the backbeach. Representative surface sediments were taken at 16 cobble stations from an enclosure of about 1 m^2.

The transverse profiles and the sampling stations in each profile were outlined on the orthophoto shown in Figure 2.

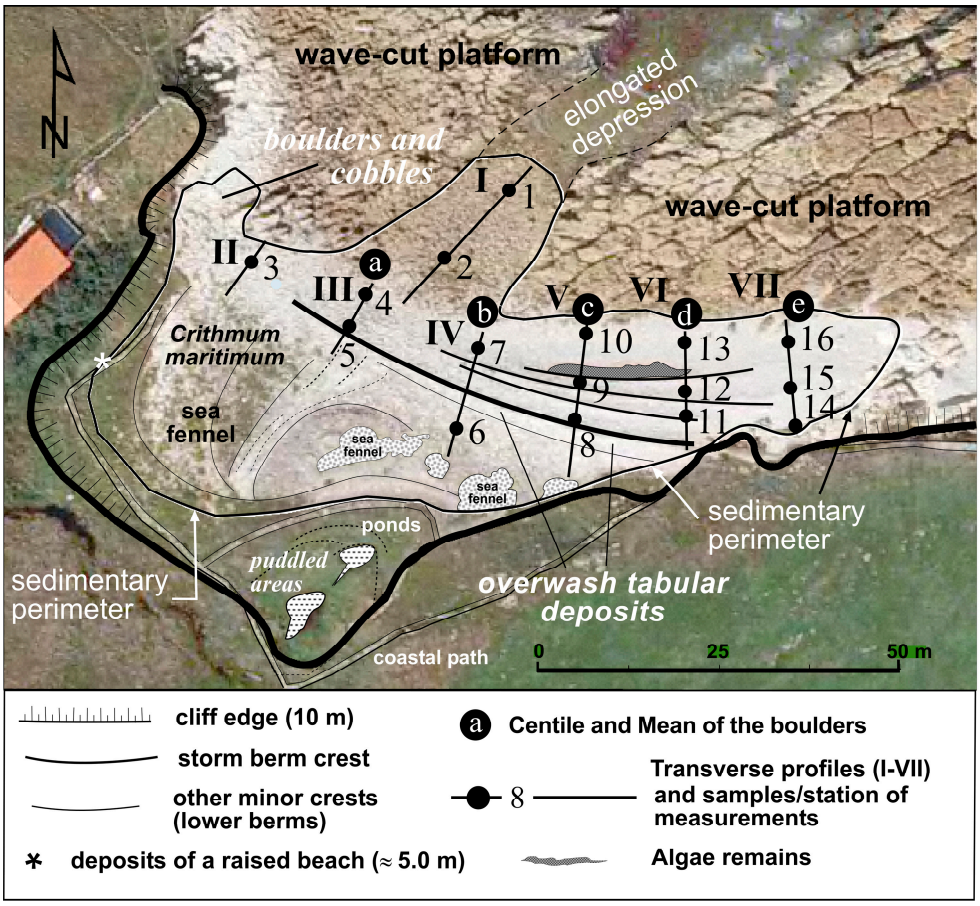

Figure 2. Perimeter enclosure of La Maruca/Pinquel beach redrawn on the 2023 image obtained from [29]. The cobble deposits rest on the substrate of jointed limestone, with square and rectangular plans. All 16 samples, taken on the transversal profiles (I–VII), can be observed, including centile and mean size of boulders (**a**–**e**) and the crests of the identified berms.

3.2. Field Campaign

Several preparatory visits were conducted to better understand the characteristics of the beach. For direct measurements, two consecutive days were required. Field surveys were thus conducted on 22 and 23 March 2023. Low tides were recorded at 0.146 m on the first day and 0.198 m on the second [31], during a period of calm wave conditions and spring tides (Figure 2). Direct measures were needed from 7:30, after the high tide, to 18:20.

Once on the beach, cross-sections were located, and stations were located and transferred from the 2023 orthophoto and slightly modified where appropriate.

The beach morphology was obtained in a very easy manner using a low-cost technique [32–34]: the slopes on the surfaces were recorded with a standard clinometer (in this case, using a conventional mobile phone), and the lengths were measured with a conventional measuring tape. A comparison between the measurements taken with the tape and those extracted from the 2023 orthophoto indicated a minimal discrepancy. The segments follow one another until each profile is completed. The upper storm crest, the stepped berms, and the overwash lobes and sheets can be distinguished by measuring their length, width, and height as well as representative beach slope angles from the foreshore belt and upper beach to the inner backbeach. Representative surface sediments (16 cobble stations) were randomly taken in situ from an enclosure of about 1 m^2, two stations along the elongated depression (1,2) and one (6) in the backbeach. Boulder samples were taken

at the lower side of the profiles (III: a to VII: e), and their intermediate axis was measured (Figure 2). Furthermore, widely developed imbrications on the shore surface were verified.

3.3. Characterization of Granulometric Parameters

Particle size parameters are useful indicators to deduce the origin, transport, and depositional environments of the sediments; average and sorting are those of greater importance [35].

The different cross-shore size–shape zonation is evident on gravel beaches [36], but is not particularly pronounced on this beach.

Following [32], whose methodology is widely accepted, the intermediate axis of a minimum of 40 clasts at each station was measured to establish the grain size parameters of the deposits. The lengths of representative diameters or axes (a: L = long; b: I = intermediate; c: S = short) were determined, and the inscribed major and minor diameters were also measured with the aid of Vernier calipers [37,38] for each clast (Figure 3).

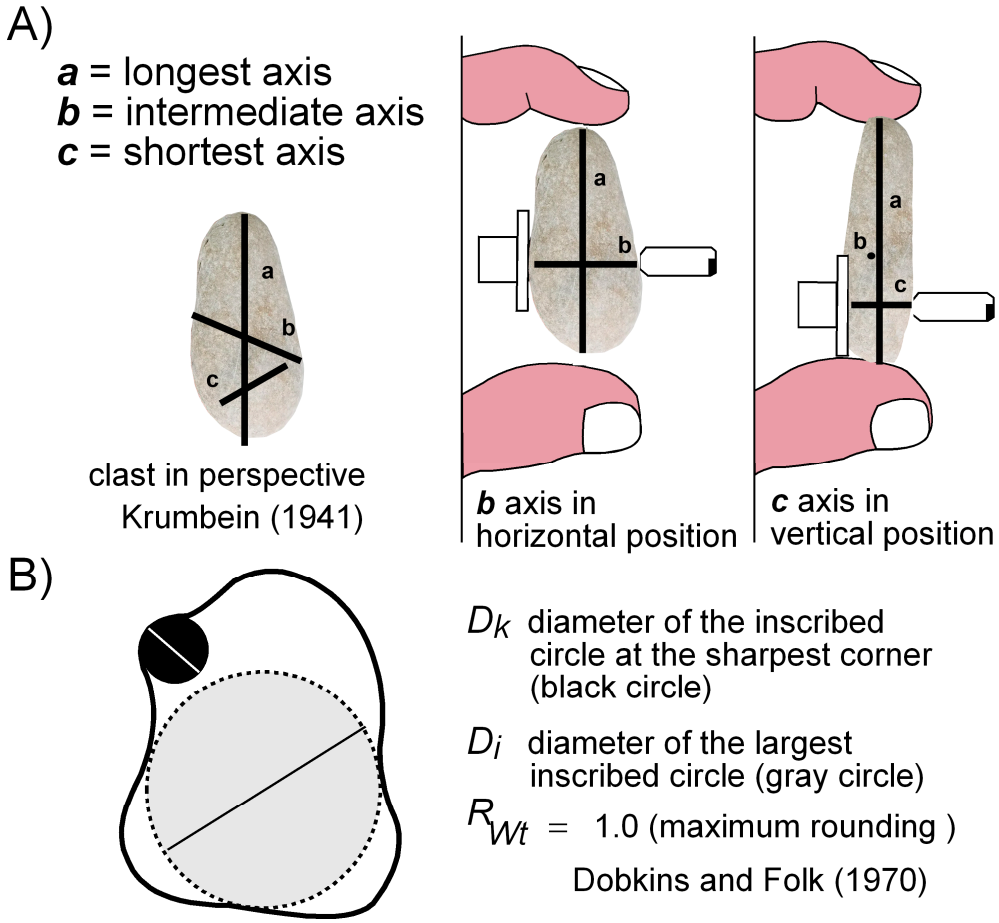

Figure 3. (**A**) Principal axes (a, L: longest; b, I: intermediate; and c, S: shortest) of a triaxial ellipsoid for an approximate particle shape. (**B**) Two-dimensional particle image showing definitions for the minor diameter (black) and the maximum inscribed circle (gray).

Two widely accepted methods were used to analyze clasts. The grain-size parameters were calculated following the method in [4], who proposed a graphic method based on the cumulative grain size distribution curve, and represented as isolines (trend maps) on the 2023 orthophoto. These parameters are centile (1% coarsest size) or the size of the largest particles in the sample, mean (Mz), sorting (σI), skewness (SkI), and kurtosis (KG). The statistical analyses were performed using the software GRADISTAT [39]. The centile

is considered important because of its great affinity with the mean, which is particularly useful when the mean values vary only slightly [40].

3.4. Shape of Particles

The shape index (roundness, sphericity, and oblate–prolate index) is used to characterize the morphology of sedimentary particles [38]. On beaches, sphericity is less prominent than rounding, and the oblate–prolate index becomes more negative, which is characteristic of disks. The authors of [38] report flattened ("oblate") beach gravels with medium-to-low sphericities (0.60). The geometry of the particles exerts a significant influence on their hydrodynamic behavior during transport [41]. The oblate–prolate index (OP) is based on the relationships between the major axis and the intermediate and minor axes (L–I/L–S) (Figure 3A). The rounding index is obtained by measuring the diameters of the smallest (Di) and largest (Dk) circumscribed circles (Figure 3B) in each clast (RWt = Dk/Di).

Sphericity establishes the shape of a particle in relation to a sphere of the same volume, regardless of its size. In a two-dimensional analysis, the authors of [42] calculated the maximum projection sphericity, which is represented in four geometries: sphere (1.00), rod or cylinder (0.74), blade (0.61), and disk (0.54). As illustrated in Figure 3, the four extreme shapes—a blade, a rod, a spheroid, and a discoid—can be calculated from the long (L), intermediate (I), and short (S) orthogonal axes.

The values of each granulometric parameter, i.e., centile, mean, sorting, skewness {asymmetry}, and kurtosis, and particle shape parameters, i.e., roundness, sphericity, and oblate–prolate of the surface sediments, were obtained for each station and plotted on the orthophoto of 2023. Subsequently, trend maps including the class values were manually drawn [40,43] and so were the main isolines proposed by several authors. In [44], the authors state that changes in the parameters' location contain information about sediment transport patterns. Manual interpolation has been successfully employed in a variety of coastal settings, including embayed, sandy, and gravelly beaches, as well as small coastal dune fields. Initially, automatic interpolators were utilized; however, these were subsequently dismissed due to their tendency to generate interpolations that lack authenticity.

3.5. Analysis of Coastal Dynamic Agents

A mutual relationship is established between the dynamic coastal agents (waves, tides, and currents, mainly represented by longshore currents) [45] and the coastal morphology and sedimentation, in this case, in a cobble beach [10]. These agents trigger short-term transport and deposition processes, such as waves and tides, and long-term processes, such as sea level [46,47]. The aim of the present work is to establish the relationship between cause (wave incidence: the NW direction) and effect (bar and berms orientation: NW–SE).

The following sections present a summary of the characteristics of the coastal dynamic agents that affect the study area.

3.5.1. Waves

Waves represent the most important energy factor in the short term in the modeling of any type of beach. Regarding the distribution of sediments in both, the construction stages (mainly during calm periods) and the erosion episodes (mainly during storms), which are articulated in the short (seasonal or cyclical) and in the long term, with the intervention of sea-level rise. Active gravel beaches are located on coasts exposed to the attack of waves, although this is not the primary condition for their formation, but rather the sedimentary contribution to the coastal edge of suitable volumes and fractions.

Wave characteristics, in statistical terms, were obtained from the SIMAR point 3136036 (Figure 4A), a database elaborated by [48]. The SIMAR dataset is made up of time series of wind and wave parameters obtained from numerical modeling. It is important to note

that the nature of these data is simulated and not derived from the direct measurements of natural phenomena (Figure 4B).

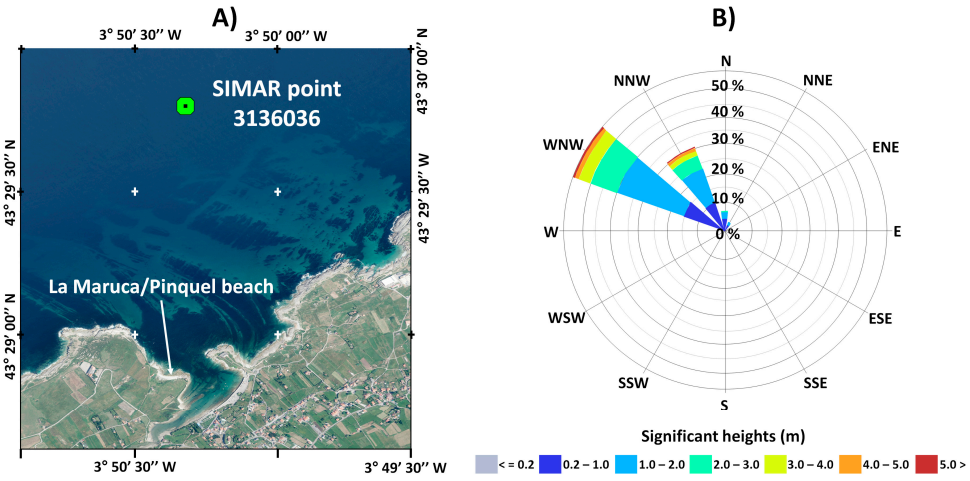

Figure 4. (**A**) Location of SIMAR point 3135036 (NNE of La Maruca/Pinquel) presenting the most representative parameters of the incoming waves. (**B**) Wave directional rose and significant heights (1958–2024), with those from the WNW and NNW dominating (modified from [48]).

Large ocean swells generated in the North Atlantic Ocean can reach up to 10–12 m in significant wave height (Hs) with a mean value of around 2 m and an average annual maximum of around 6 m. The peak wave period ranges between 8 and 15 s [49]. Incoming waves near the La Maruca/Pinquel arrive from the main direction WNW and NNW (Figure 4). The waves are refracted about 90° to the right (dextrorotatory sense) to penetrate frontally over deposits of the ridge. When oblique waves occur, gravel clasts can be transported along the shore [50].

3.5.2. Tides

The contribution of the storm tide is more significant as it exploits the depression (direction) to channel the deposits from the shore surface to build the lobe (the SW area of the backbeach). A detailed study of storm surges (meteorological tides) and astronomical tides lies outside the scope of the present work.

Sea-level surface measurements and those related to tidal oscillations were obtained from the tide gauge located at the western mouth of the Bay of Santander (latitude 43°27′40″ N and longitude 03°47′26″ W).

The astronomical tides on the Cantabrian coast are semidiurnal and mesotidal (based on the main lunar component M2). The average range is 2.8 m with maximum values that can reach 5 m of high spring tide height or even exceed this value, and that tend to increase toward the Basque Country. The average monthly and annual ranges available show an average value between 2 and 4 m (mesotidal) in 70% of the cases, below 2 m (microtidal) in 20%, and above (macrotidal) in the rest [51].

A wide range of variability translates into an extended area in which waves can affect the shoreface resulting in macrotides [52]. The increasing tidal range induces shoreline mobility on both the wave dynamics and the resulting morphodynamics [53].

3.5.3. Sea Level

Sea-level rise is a mechanism indirectly influencing gravel barrier migration landward, considering that storm intensities operate independently of sea-level change. Between 1993 and 2019, the mean sea level in the Cantabrian Sea rose at a rate of 2.46 ± 0.43 cm dec^{-1} (rates per decade = dec^{-1}); from 2004 to 2013, this rise somewhat decelerated [54].

Extreme events contribute to the increase in average sea-level rise due to the combination of strong winds and storm surges with astronomical tides, resulting in coastal overtopping. These meteorological tides occur under the combined action of low atmospheric pressures, associated with the passage of storms, with wind drag. Under these conditions, sea-level rise reaches 30–40 cm [55]. In the Cantabrian Sea, this occurs once every 50 years, with maximum values close to 0.5 m, showing that changes in the climate system are faster than initially thought [56].

4. Results

4.1. Geomorphological Mapping on the Basis of Historical Orthophotographs and Fieldwork

A geomorphological map of the study area could be obtained thanks to the mapping of the geomorphological features on various orthophotographs in conjunction with the fieldwork (Figure 5).

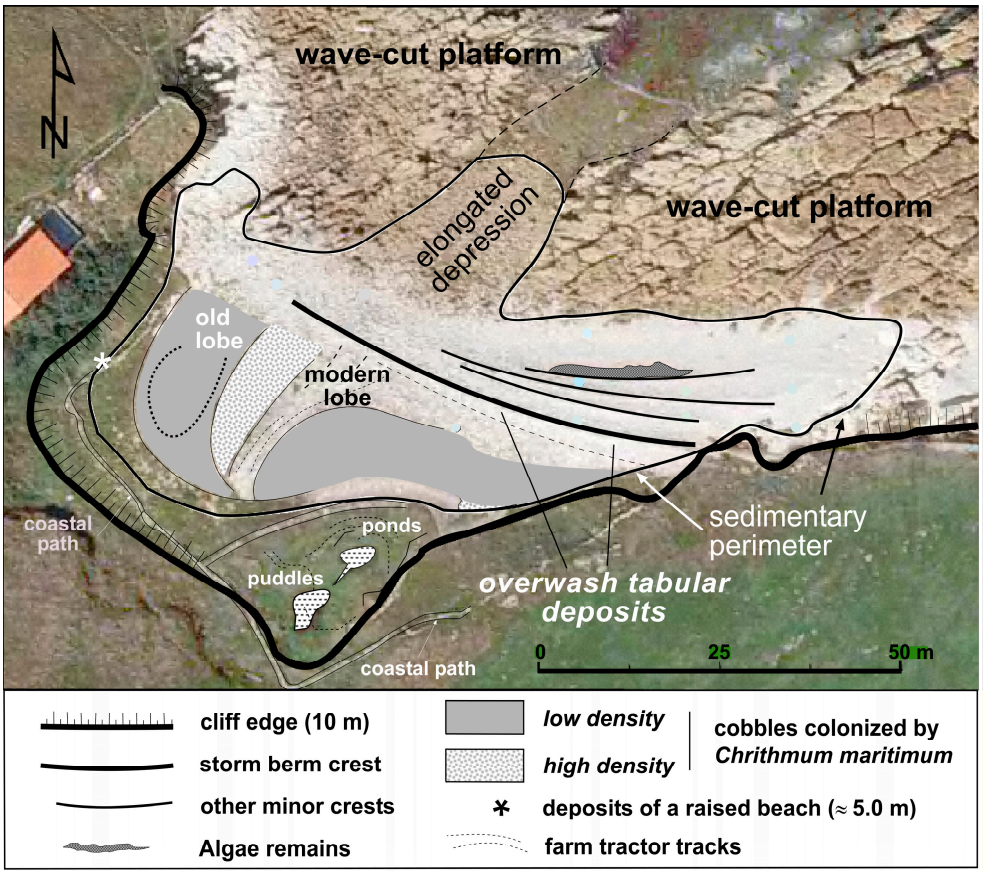

Figure 5. Simplified cartography of La Maruca/Pinquel beach and its surroundings based on 2023 orthophoto (image obtained from [28]).

The morphological parameters that were mapped include the perimeters and surfaces covered with deposits; the position and length of the berm crests; some morphosedimentary units, such as overwash sheets and lobes; and, as an approximation to the dynamo-sedimentary inactivity, the vegetal colonization.

La Maruca/Pinquel cobble beach is a typical embayed or headland-bay beach developed on a rocky coast [53]. The beach does not experiment any transfer or loss of sedimentary volume given that its deposits are confined to a rocky enclosure (Figure 5). In this type of beach, known as perched beach, changes only occur within itself and on its periphery.

La Maruca/Pinquel beach plane shape is irregularly rectangular. This beach was formed on a broad rocky cove of about 9000 m^2 presenting a rectangular plan-oriented NW–SE, 40 m wide on the western side. Cobbles are widely colonized by sea fennel (*Crithmum maritimum*) in an 18 m wide area on the eastern side for about 100 m, in an almost W–E direction. The beach is slightly arched with a slightly concave arc in plan of 95 m, pointing NE (Figures 5 and 6A,B), over a depositional surface less than 3100 m^2. It also reaches a maximum height of just over 5 m where the crest of the ridge extends. An irregular wave-cut platform was carved with prismatic joints. This platform widely outcrops in the lower intertidal zone, rising just over 1 m from the bottom.

On the southwestern side of this beach, a heterogeneous beach deposit is preserved; this consists of subangular and rounded pebbles and cobbles, with a matrix of coarse sand with both fragments and whole shells, mostly limpets (*Patella* spp.). This composition is similar to that of the Dunkirkian deposit, cited in [57] for Bikini beach, which hangs at an approximate height of 5 m.

The deposits occupy a lower beach step with respect to the wave-cut platform, their appearance is rather flat, and their morphology is consistent with the geometry of a prism. This step is separated from the back cliffs, which are 10 m high and remain unchanged toward the N. The southern backbeach is devoid of gravels, and some ponds of subcircular contour and puddled surfaces (Figures 5 and 6A) of karstic origin can be observed, covering an area of about 375 m^2.

At the foot of the tidal rocky surface, a loose channel-shaped depression has been excavated perpendicularly to the low tide level and is covered by clasts; during low tides, water is drained out of the depression (Figure 6A). This presents an elongated NE–SW direction, about 41.5 m long with variable widths, between 11 and 17.5 m, narrowing seaward with a very small slope. It is incompletely filled with cobbles colonized by green algae (*Enteromorpha* spp.) and intertidal fauna: limpets (*Patella* spp.), small gastropods (*Melarhaphe neritoides*, *Gibbula* spp., *Littorina* spp.), barnacles (*Chthamalus* spp.), marble crab (*Pachygrapsus marmoratus*), etc., evidencing a great dynamic inactivity only interrupted by storms (Figure 6A).

The area in which the abovementioned deposits accumulate exhibits a simple geometry, characterized by an asymmetrical ridge configuration (Figure 6A,B), with a large permanent bar or berm crest arched WNW–ESE (Figure 6A–D). The area draws a concave transverse profile in the foreshore, where slopes are steeper (maximum of 30º in profile IV); from the upper crest, the backbeach surface gently slopes landward (Figure 6B). The deposits are embedded in the wave-cut platform, whose culminating surface is irregular and rises less than 2 m high (Figure 6F,G). The limiting belt of the rocky bottom with the lower deposits of the foreshore presents heavily worn surfaces (polished limestone), with bare sections alternating with sections covered by cobbles (Figure 6F,G).

Overwash lobes have contributed clasts (less than 0.75 m thick; 20 m long; 12 m wide) to the western area of the beach. These have been placed during different episodes and represent a type of deposit that erodes the crest of the upper berm with no return to the foreshore [58]. The westernmost lobe shows a subcircular contour (20 m long; 18 m wide) and is colonized by fennel. Attached to its eastern side, another longer, narrower, and more modern lobe migrated landward and stabilized (Figure 5).

Along the eastern area, the backbeach from the upper crest is a simple gentle slope presenting the overwash deposits, which have acquired a tabular geometry. Cobbles subject to continuous water mobility acquire a light gray tone in their surface (Figure 6B,D,G). These deposits are distributed along the upper foreshore and outer backshore, upper berm, and overwash tabular prisms and lobes. Cobbles inactive for long periods acquire a medium gray tone in their surface (Figure 6C) under subaerial conditions, stabilizing on the

leeward side of the bar and on the overwash lobe. Numerous clasts contain millimetric-scale bioperforations caused by certain species of bivalves, polychaetes, and even sponges.

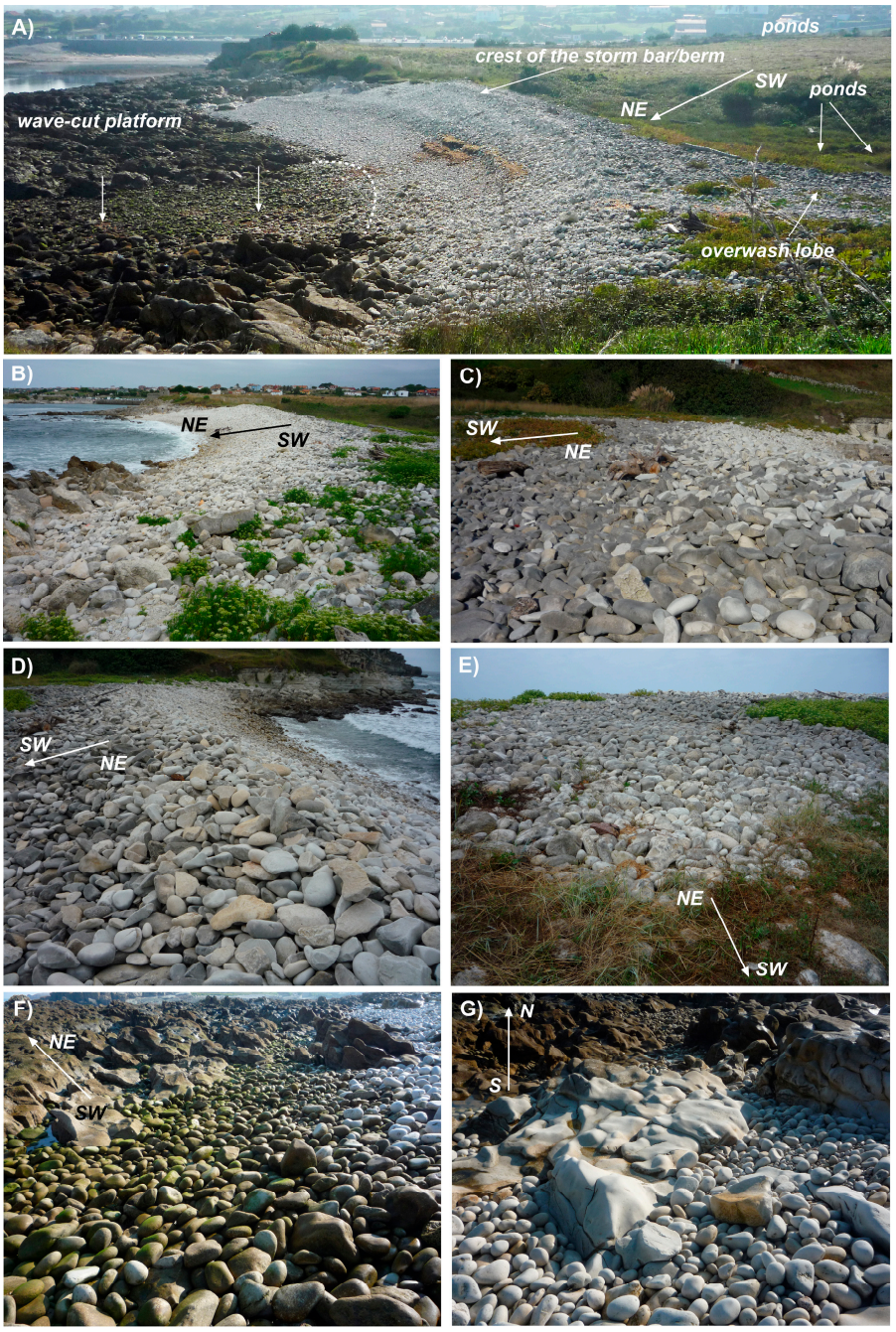

Figure 6. (**A**) Panoramic view of La Maruca/Pinquel beach from the NW. Several berms can be identified; the lower ones retain algae remains and resemble recessed steps. The channel-shaped depression, embedded in the rocky platform that rises just over 1 m high (left side of the photo), can be appreciated (sampling stations 1 and 2, marked with arrows). The overwash lobe is identified on the right bottom corner. (**B**) Thickest deposits (mainly boulders) of the northwestern corner. (**C**) On the leeward side, active (light gray) and inactive (medium gray) cobbles coexist. The leeward slopes range from 7° at the crest to 11° and 13° at the foot (most internal). (**D**) Detail of the crest (upper berm) and the arrangement and degree of wear of the cobbles, seen from the eastern side. (**E**) Front area (inner) of the overwash lobe a few decimeters thick. (**F**) Boundary belt at the foot of the foreshore, presenting a worn rocky substrate and imbricated cobbles, many covered with green algae. (**G**) Highly polished rock outcrop, indicative of the abrasive power of the cobbles, where sedimentation is low.

The largest clasts of the study beach are found in the western foreshore (Figure 6B) and between the foot of the intertidal zone and the rocky bottoms. These clasts are characterized by the maximum centile and mean size (Figure 6A) and are represented by boulders (Figure 6B), and many are colonized with green algae, which indicates their immobility for most of the time. They are located and remobilized during storm surges, as contemplated by the [19] model for Sker-type beaches.

In almost all tidal zones of La Maruca/Pinquel beach, cobbles are arranged in a clear and wide imbrication structure (Figure 6E,F) dissimilar to those restricted to the upper part of Sker beaches [19] and to the foot of storm berms [59].

Sediment volume increases from transversal profiles II to IV (Figure 7); most of the deposit is concentrated in the central foreshore, profiles IV, V, and VI; sediment volume then decreases toward the eastern edge, profile VII. On this rocky side, small and isolated accumulations of pebbles are installed, produced under strong waves.

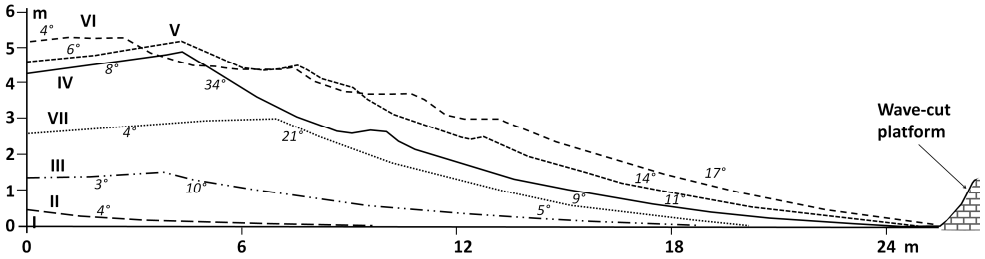

Figure 7. Superposition of the seven simplified transversal profiles and representative slopes, whose feet connect with the abrasion platform at a very worn strip, which hangs at a height below 2 m. The beachface is steeper in profiles IV, V, VI, and VII and is reflective.

Down the foreshore, a series of highly variable lower berms are staggered, in a maximum number of three (45 m, 37 m, and 25 m), and are built during the spring and neap tides, with the concavity softening toward the southeastern corner (Figure 6B,D and Figure 7). The cross profiles reveal the maximum height and volume of cobbles in profiles IV, V, and VI, where the berms are built (Figure 7).

These berms are asymmetrical, culminating in a main crest whose slope is greater on the seaward side due to the greater energy (larger grain sizes) developed by the waves in the swash under reflection conditions, especially, in the case of a stormy episode. In the backwash, energy is lost due to water infiltration resulting from previous wash [60]. The main crest culminates at heights slightly higher than 5 m and widths of around 1.5–2.0 m, while the tide berms present maximum heights of 1 m and are less than 1 m horizontally (Figure 7).

Swash and backwash are the most important processes along the foreshore, with swash representing the most powerful of them. Swash infiltration is probably the dominant factor in the control of the beachface gradient [60]. Formation of berms is enabled by the spring and neap tides bringing swash to a relatively long halt [61].

The slopes are higher in the upper foreshore, showing some segments with erosion slopes, which gradually decrease toward low tide and draw a clear concavity seaward. The depositional slopes are high, greater in the central foreshore due to the greater energy developed by the incident waves. The average slope is about 15–20° and can reach 44° in the upper part of the berm (Figures 6B and 7) if they are the result of erosion.

4.2. Granulometric Parameters, Shape Characterization, and Coastal Dynamic Agents

The cobble deposits, characterized by grain size parameters and clast shapes, are distributed in response to the incoming waves and wave-induced currents [62] and the availability of inherited clast fractions. Both grain size distributions and particle shape are

related to beach dynamics [19,63]; these include the transport of gravel up the foreshore by wave storms to form a large berm or storm bar and overwash small longitudinal bars, overwash lobes, and storm sheets projected landward.

4.2.1. Granulometries

Surface distribution of the granulometric parameters varies greatly, although centile and mean agree better between them due to the similarity of maximum sizes (Figure 8).

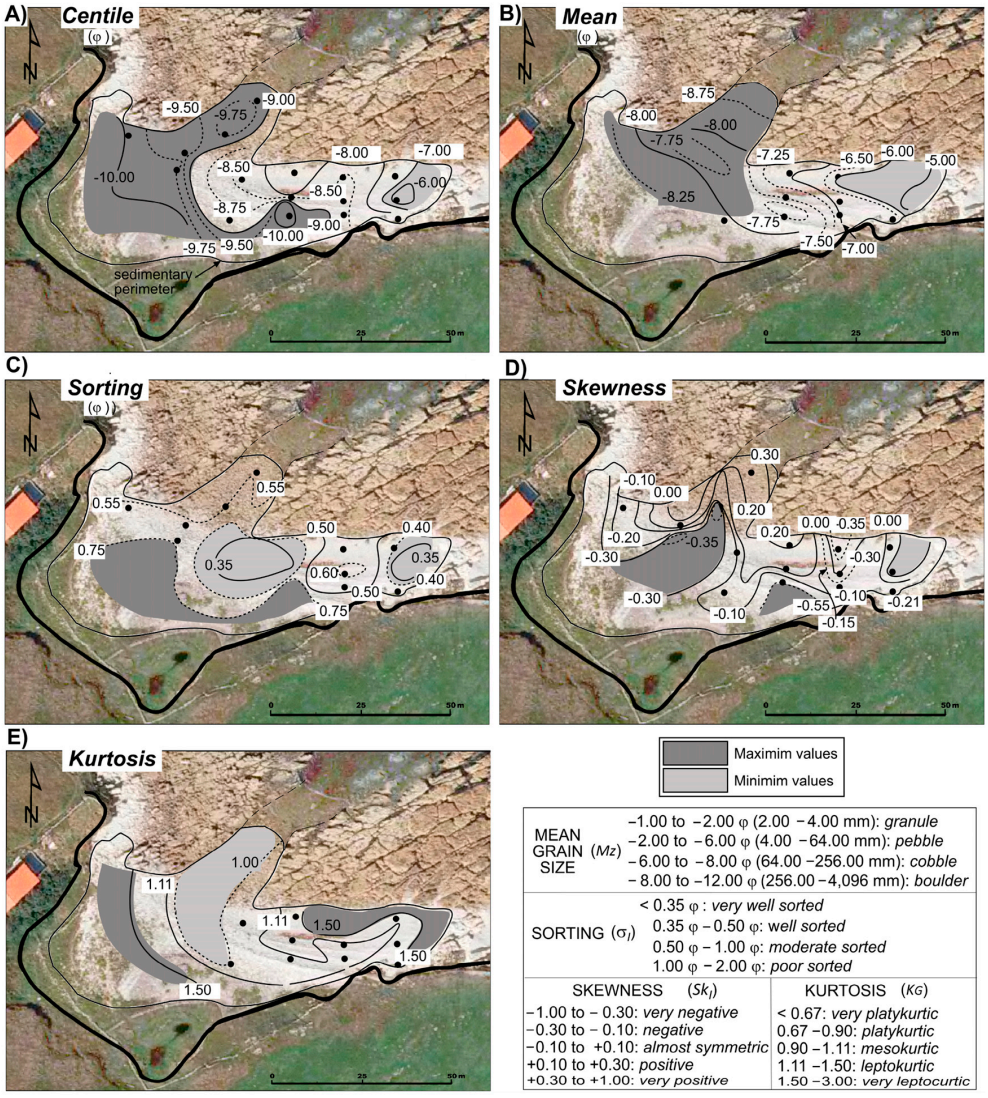

Figure 8. Trend maps of granulometric parameters: centile (*Mz*), mean (σ_I), sorting (Sk_I), skewness, and kurtosis. Class intervals for each parameter are presented.

The largest sizes are found on the western side of the study beach, represented by boulder fractions (>−8.0 ϕ), which stabilize in the upper foreshore (Figure 8A,B). Transitioning longitudinally toward the eastern side, sizes decrease, represented by boulder and cobble fractions (Figure 8A,B, respectively).

The centile and mean values for samples a, b, c, d, and e (Figure 2), given the difficulty of expressing data from the lower belt of pebbles on the trend maps (Figure 8A,B), are presented in Table 2.

Table 2. Boulder sizes (centile and mean) in ϕ units and the equivalent in millimeters, located at the foot of the foreshore near the wave-cut platform.

Sample	Centile		Mean	
	ϕ	mm	ϕ	mm
a	−9.79	890	−8.90	480
b	−10.30	1340	−9.43	690
c	−9.57	760	−8.87	470
d	−8.68	410	−7.59	192
e	−8.49	361	−7.05	132

Cobble sorting varies from extraordinarily very well sorted (0.30 ϕ) to very well sorted (0.35 ϕ) and moderately sorted (0.75 ϕ) on the western and southwestern sides of the beach (Figure 8C). A longitudinal variation W–E from higher to lower values can be deduced. In the western area of the beach, sorting is very good at the lower half of the foreshore, probably due to the energy of the incoming waves through the rocky depression.

As for skewness, the most negative values can be located in the western side, with positive values gradually concentrating toward the eastern corner (Figure 8D). Angularities (KG) of the curves (peakedness) are distributed from the most acute (>1.50), surrounding the perimeter of the intertidal zone, to medium values (around 1.10) in the middle and lower foreshore (Figure 8E); in this sense, the most remarkable finding is the lack of flat curves.

In the case of the centile, data obtained for the boulders in the lower intertidal zone, linked to profiles III to VII, were included in the present work. The areal transitions of the parameters are related to the incidence of waves and the results of the transverse and longitudinal distributions of the sediments [64] because of the transport processes that also involve morphological reconstruction.

4.2.2. Particle Shape

Coastal gravels are washed repeatedly by waves, and they can therefore present very rounded shapes. The maximum possible rounding was recorded only in a few clasts in the study beach. Average rounding in clasts located at each station are relatively high, with values ranging from 0.70 to 0.75, and distributed throughout the western area. Minimum values (<0.6) are observed in more restricted surfaces toward the opposite side of the study beach. A simple longitudinal transition toward the E can be interpreted (Figure 9A).

The results obtained in the present work show what, according to sphericity, are perfect rods on the southwestern edge, with maximum values of 0.74, transitioning longitudinally to perfect disks toward the N and the southeastern corner: 0.54 (Figure 9B).

A more complex distribution is obtained when considering the oblate–prolate index (*OP*), with results reaching extreme values in accordance with the definition proposed in [39]. Maximum values (0.0 to +0.5) are found in the southwestern half of the study beach, coinciding well with the maximum values of sphericity (rods and blades), while minimum values (−5.0) are distributed toward the N and NE, nearly at the lower tidal edge (Figure 9C).

The abundance of disk-shaped clasts responds to the dominant back-and-forth abrasion in which, once the last wave breaks on the beach surface, waves are resolved as a sheet of water of centimeter-to-decimeter thickness, which ascends landward (“swash”) and continues along the immediate descent (“backwash”). This can be favored by a sandy fraction, which acts as additional abrasive material.

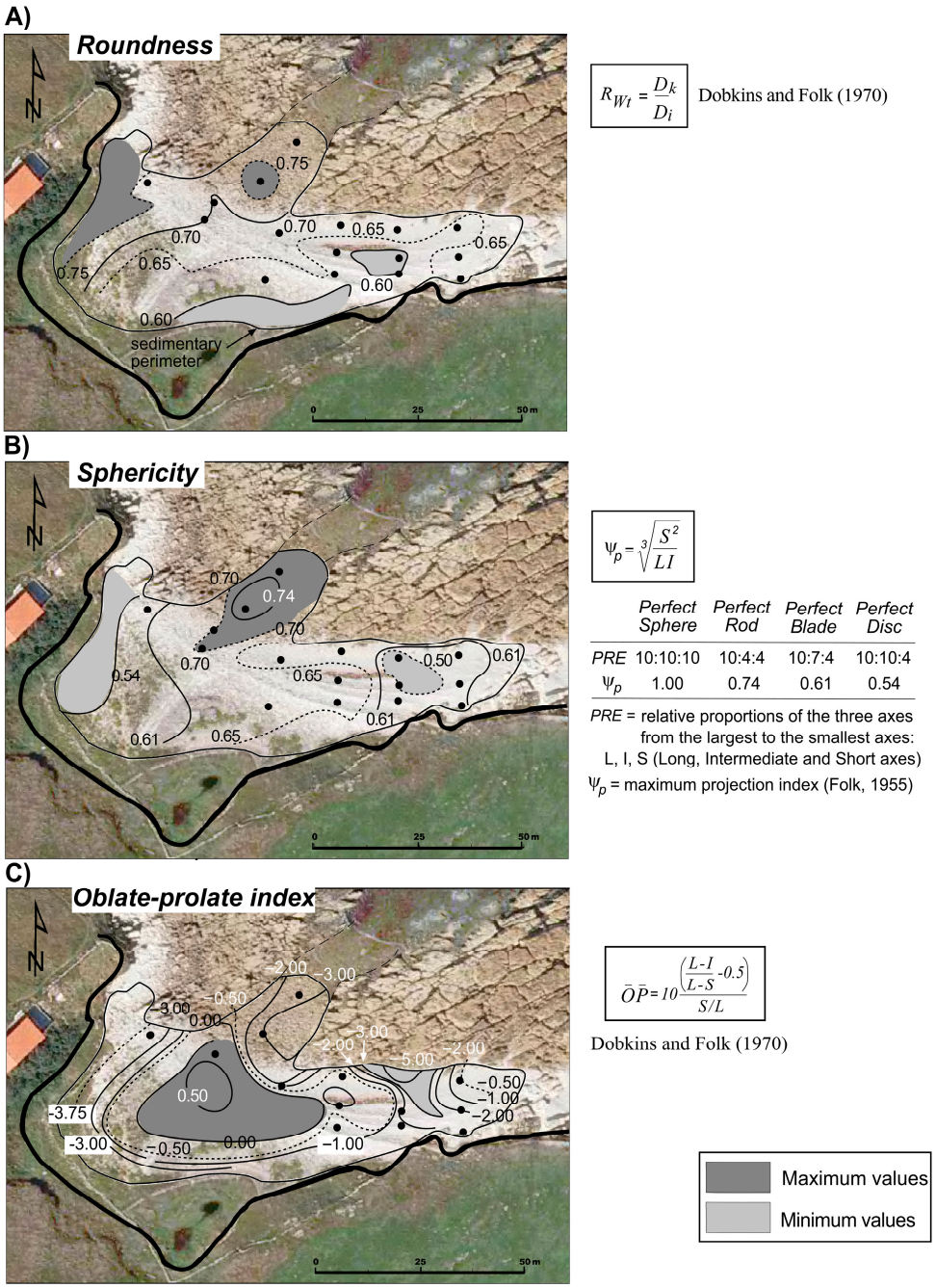

Figure 9. Trend maps of averaged particle shape parameters: (**A**) roundness [38], (**B**) sphericity [42], and (**C**) oblate–prolate index [38].

4.3. Morphosedimentary Beach Evolution from 1984 to 2024

The morphological and sedimentary evolution of La Maruca/Pinquel beach since 1984 has depended closely on dynamic changes resulting mainly from wave action (Figure 4B), a process that normally occurs in sandy beaches [65,66]. These changes affect a mesotidal and sometimes macrotidal area, following storm and calm wave cycles [67] in a seasonal periodicity in accordance with wave climate. These processes have been simplified as follows: in winter seasons, characterized by storm waves, erosive processes dominate; in summer seasons, characterized by calm waves, swells reconstruct the equilibrium profile of the beach [63].

The current perimeter of La Maruca/Pinquel beach is composed of rocky surfaces with an almost rectangular geometry plane shape between low cliffs with greater slopes northward and subhorizontal in the lower belt affected by the tides.

Morphological variables manifest themselves according to a seasonal cyclicity in the direction of the wave fronts and the gradients in wave energy [68]. Sedimentary characteristics, mineralogical composition, shape and granulometric parameters, and beach slope are involved [69]. The exposed front of the beach is mainly controlled by the larger size of the sediment and the intensity of the wave action [70], which translates into greater energy. On sandy beaches, a direct relationship is evident between beach slope and average grain size in the intertidal sector. Grain size increases with increasing slope, and the beach is more exposed to the energy of the incident waves [71]. In gravel beaches, this equivalence is far from being closely matched and so is the relationship between the dynamic changes and the resulting morphology [72].

The active surface where the movement of gravel occurs can be temporarily identified using the contours that define where the water sheet arrives as a result of tidal variations dominated by the back-and-forth processes; this area can also be determined by the deposit transfers to the rear areas that storm waves cause through overtoppings.

Two varieties of overwash deposits can be differentiated in La Maruca/Pinquel beach; the simplest type is tabular, and these deposits present widths from 1 to 2 m up to a maximum of 5 m, over a length of 60 m. Within this belt and along the entire leeward side of the upper berm crest, smaller and unmappable longitudinal bars are present, showing heights less than 0.35 m and lengths less than 1 m and configuring a finger-shaped or comb-shaped morphology. Toward the W, this belt is replaced by an area where overwash lobes are installed. An isolated wide washover lobe that reached a surface of 225 m^2 can be observed in the 2020 ortophoto, in what is supposed to be a concentrated sedimentation during wave storms that migrated landward. Also, of note is the gradual colonization of the western and southern corners of the study beach by sea fennel, indicative of a temporary sedimentary cessation.

The arching of each crest suggests the incidence of waves and their adaptation to the beach surface; here, the most frequent wave trains are from WNW and NNW (Figure 4B), turn toward NE, and break until they dissipate in the foreshore. The inner berm is represented in all records given its great magnitude, with heights lowering toward the lateral ends and downward. This berm usually develops an erosive front in the upper belt of the crest and remains almost invariable in the long term, while the tendency for the lower berms—given their dependence on tidal cyclicity [61], the angle of the incoming waves, and the parameters of height and period [73]—is to disappear, with new berms being created. In some cases, lower crests are attached to the inner one, due to a change in the incidence of the waves (Figure 10B). Two clear events could also be detected in the orthophotos; in these episodes, the upper front of the eroded bar generated a scarp (about 0.4–0.5 m) up to 45° from the crest to the foreshore in 2014 and 2020 (Figure 10E,G, respectively).

The surface coated with cobbles followed very irregular patterns in 1984, covering a minimum area of 2910.2 m^2 (Table 3; Figure 10A) with a backbeach width of 42.3 m, greater in the southeastern corner and did not exceed 3058.3 m^2 between 1984 and 2010. During the last five years of this period, this area decreased to a minimum of 2177 m^2 probably due to a contraction of the deposit surface; however, it is most likely that it grew vertically. Deposits have advanced and dismantled toward the eastern side of the beach, some as isolated patches, changing irregularly from one record to another. Some rock surfaces polished by the wear of cobbles in previous stages are now outcropping (Figure 6G), occupying surfaces previously filled with cobble deposits.

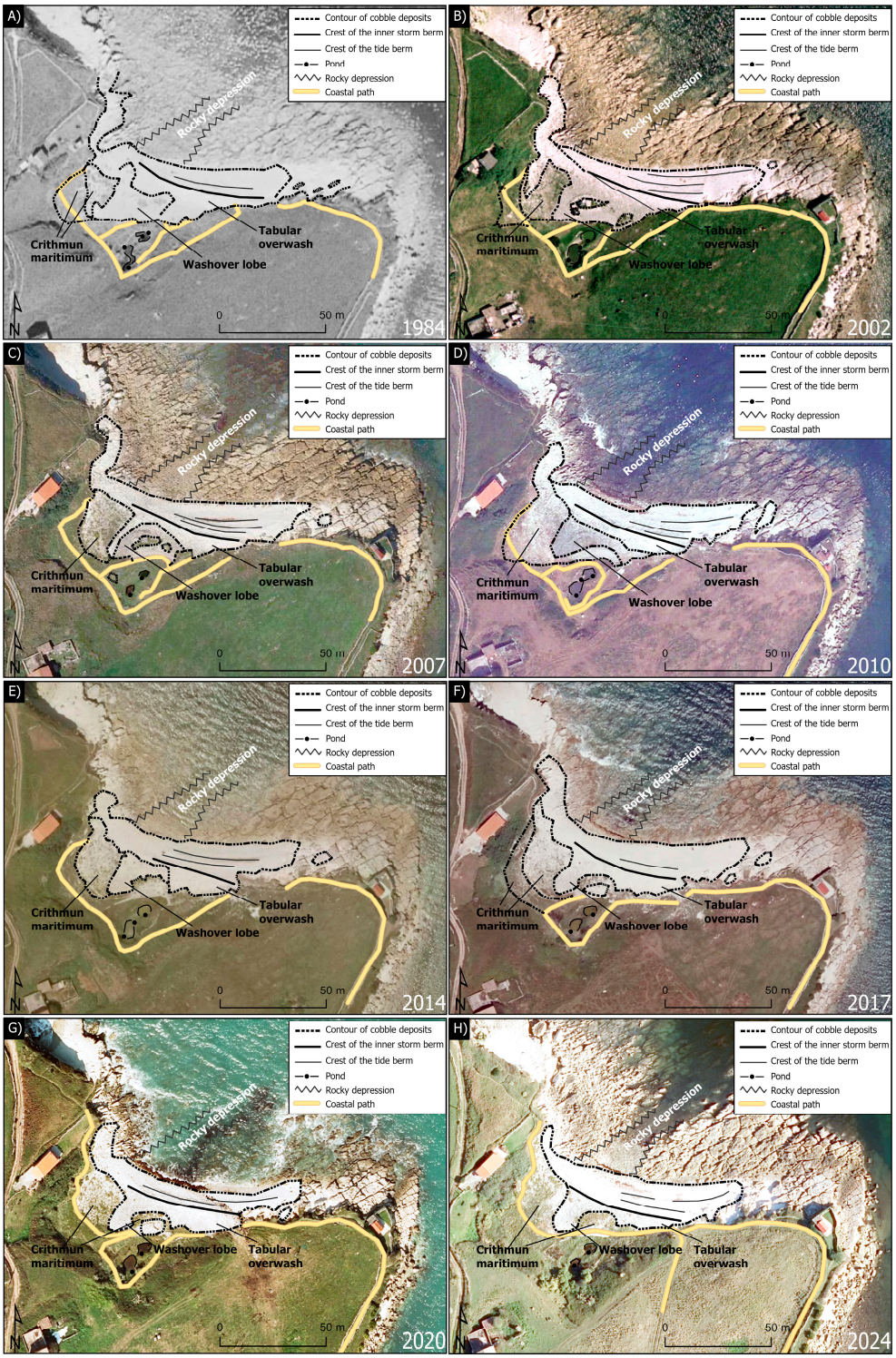

Figure 10. Mapping process applied to orthophotos from 1984 to 2024 (**A**–**H**). The following features have been identified in the orthophotographs captured at different times: contour of cobble deposits, crest of the inner storm berm, crest of the tide berm, pond, rocky depression and coastal path.

In 1984, this beach developed an upper berm with an elongated crest of 61.8 m and other minor one of 37.5 m down the foreshore (Figure 10A; Table 3). A small area at the western end was partially colonized by sea fennel (*Crithmum maritimum*). Landward of the upper berm, overwash tabular sheets drew an elongated triangular plan; this was repeated, with variable widths, generally increasing eastward, in the most recent records.

Table 3. Surfaces covered with clast deposits and berm crest number, length, and maximum distance between crests. Data are completed with observations of interest. Information is based on orthophotos from 1984 to 2024. Length of the upper berm in bold and italics.

Year	Surface Containing Deposits (m^2)	Number of Crests (berms)	Crest Length (m)	Distance Between Crests (m)	Observations
1984	2910.3	2	37.5–***61.8***	4.2	SW fixed vegetation
2002	3058.3	4	49.4–36.2–25.9–***54.3***	3.7–4.1–3.1	Overwash in the backbeach
2007	2795.2	4	29.5–41.9–31.3–***53.1***	2.8–2.5–3.4	Fixed backbeach
2010	3032.5	4	34.1–29.2–20.8–***55.2***	4.5–2.8–2.3	Well-developed berms
2014	2437.4	3	40.5–34.0–***39.9***	3.1–4.3	New lobe
2017	3114.3	2	27.6–***50.9***	4.6	Active overwash sheet and lobe
2020	2177.0	3	33.3–39.4–***54.3***	2.4–2.8	Upper crest erosion
2023	2314.7	3	52.3–47.5–***48.4***	5.07–2.8	Lobe is inactive
2024	2449.5	3	42.9–30.5–***55.2***	4.4–4.2	Lobe is fixing

The number of minor crests formed in the study beach usually varies throughout records since these features are ephemeral forms, although a frequency of two or three units can be appreciated. In records showing more than three berms, the upper crest is tangentially attached to the immediately lower berm and generated high tides during spring, from approximately the middle of the beach. The third crest, lower than the second one, is also somewhat longer (Table 3).

A first overwash lobe formed in 2007 in the western area of the beach, acquired an elongated shape perpendicular to the coastline from the backshore side of the upper berm, with a surface of 278.8 m^2. The inner portion of this lobe presents an elongated subelliptical plane shape laterally linked in total continuity with the tabular overflows on the eastern side of the beach (Figure 10C). Another lobe can be observed in the same position and with similar dimensions (Figure 10G,H). In 2020, a storm sheet was generated at the eastern end of the beach, covering a larger area (192.88 m^2) than those of the previous and subsequent ones (Figure 10G).

Fixation by vegetation, mainly sea fennel, had already begun during the late years of the 20th century (Figure 10A), particularly in the western corner. The absence of clast contributions to this shadow area favors a greater colonization density by plant fixation, which is increasing gradually.

5. Discussion

5.1. Sedimentary Source Areas

The origin of La Maruca/Pinquel beach cobbles can be found at a close location linked to the retreat of the cliffs where the sedimentary prism develops. This is typical of embayed beaches in the Cantabrian Sea, in which lateral sediment transfers are not possible. For the study beach, this is specially so given that its cobbles are coarse fractions whose displacement is restricted.

The most likely suppliers of sediments for this beach are the cliffs around the backbeach perimeter and the extensive highly spatial area of about 11,500 m^2. Given that these limestones share their gray compact micrite facies with the cobbles, an isotropic behavior of these is induced. However, an additional source may have been needed from the north area.

5.2. Morphosedimentary Distribution 1984–2024

A portion of the active beach deposits in the foreshore and upper backshore belt of La Maruca/Pinquel beach has been distributed mainly following a trend of clast sizes from maximums on the western side to minimums on the eastern side (Figure 8). Other

identifiable changing trends are those in particle shape parameters, such as the decreasing roundness eastward as a result of persistent albeit very weak beach drift currents (Figure 9).

During large-magnitude wave storms with long-term recurrence, as those identified in the winters of 2009–2010 and 2013–2014 (Figure 10D,E), overwash lobes were built or reactivated (Figure 6E). These covered surfaces of just over 225 m^2 and became inactive after each event. The most common and broad process was the emplacement of tabular overwash sheets that migrated landward, widening preferably in the center and southeastern side. Both morphologies clearly indicate the landward migration of the sedimentary complex but not exceeding the contours of the first photograph from 1984.

At the end of 2013 and the beginning of 2014 (just over 3 months), a sequence of wave storms produced substantial changes on the Atlantic coasts of Europe [74,75], Asturias [76], and Cantabria [77,78]. At that time, a new overwash lobe (242.74 m^2) developed at the beach and remained unchanged from 2020 to 2024 (Figure 6E).

In most cases, overtoppings occurred landward of the crest of the upper beach bar, with greater width, the further E, represented by tabular layers a decimeter thick (Figure 6A,E). In 2007, an overwash lobe was built on the western side, covering an area of 319.25 m^2 and stabilized with the rest of the backbeach surface.

A large berm is present on the inner side, and its upper front seaward built an erosive scarp in 2014 and 2020 (Figure 10E,G). Somewhat persistent lower berms can also be observed, although these are variable in number and length (Table 3), slightly increasing their length toward the E, as the deposits were transported by the beach drift. The most common process on the study beach is the construction of up to three lower berms (Figure 10D,G), showing arched crests with the concavity seaward. During neap tides, the lower berms are built, and they lie above those formed previously. Some of these lower berms could have been formed by weaker wave storms.

The beach has experienced very few anthropic interventions, although the extraction of red algae (mainly *Gelidium sesquipedale*) required the consolidation of an access path by building pebble pavements in some sections on the perimeter contour. Farm tractor tracks were visible at some point in time on the intertidal and the supratidal areas of the beach (Figure 10C,H), but they disappeared due to the sedimentary dynamics of the beach. Because of the morphological configuration of the rocky area, the eastern area is irregularly covered with cobbles in irregular depressions.

5.3. Morphosedimentary and Dynamic Model

La Maruca/Pinquel beach is formed as a result of the asymmetry of the laminar water flow (swash) from the breakers, linked to the spring and neap tide phases of the cycle [79]. Its construction required a certain period with sea-level stationing. On this beach, successive stationing, with relatively wide tidal ranges (meso- and macrotidal), enabled the preservation of several berms over a time interval.

The scarce contrast between the different grain sizes found in La Maruca/Pinquel beach, represented almost exclusively by the fractions of cobbles in the upper interval of the Udden–Wentworth scale, characterizes the construction of this beach, similar to that of the pure gravel beach model in [80]. The upper bar ("gravel ridge"), as described in [19], contains a belt of large disks with sizes ranging from 64 to 256 mm (-6 to -8 ϕ), and its berm is considered one of the distinctive morphological features of gravel beaches (Figure 11).

Given their greater variety in granulometry and particle shape, the upper (supratidal) and lower (intertidal) belts represent the only parts of the beach that can be extrapolated to the more complex Sker beach model with high wave energy [19]. Good sorting certifies that a high degree of maturity has been reached, due to the work of the waves over long periods.

Also, the average skewness (−0.14), close to symmetrical curves, and kurtosis (1.16), typical of sharp curves, suggest that this deposit is very well sorted with sedimentary clasts.

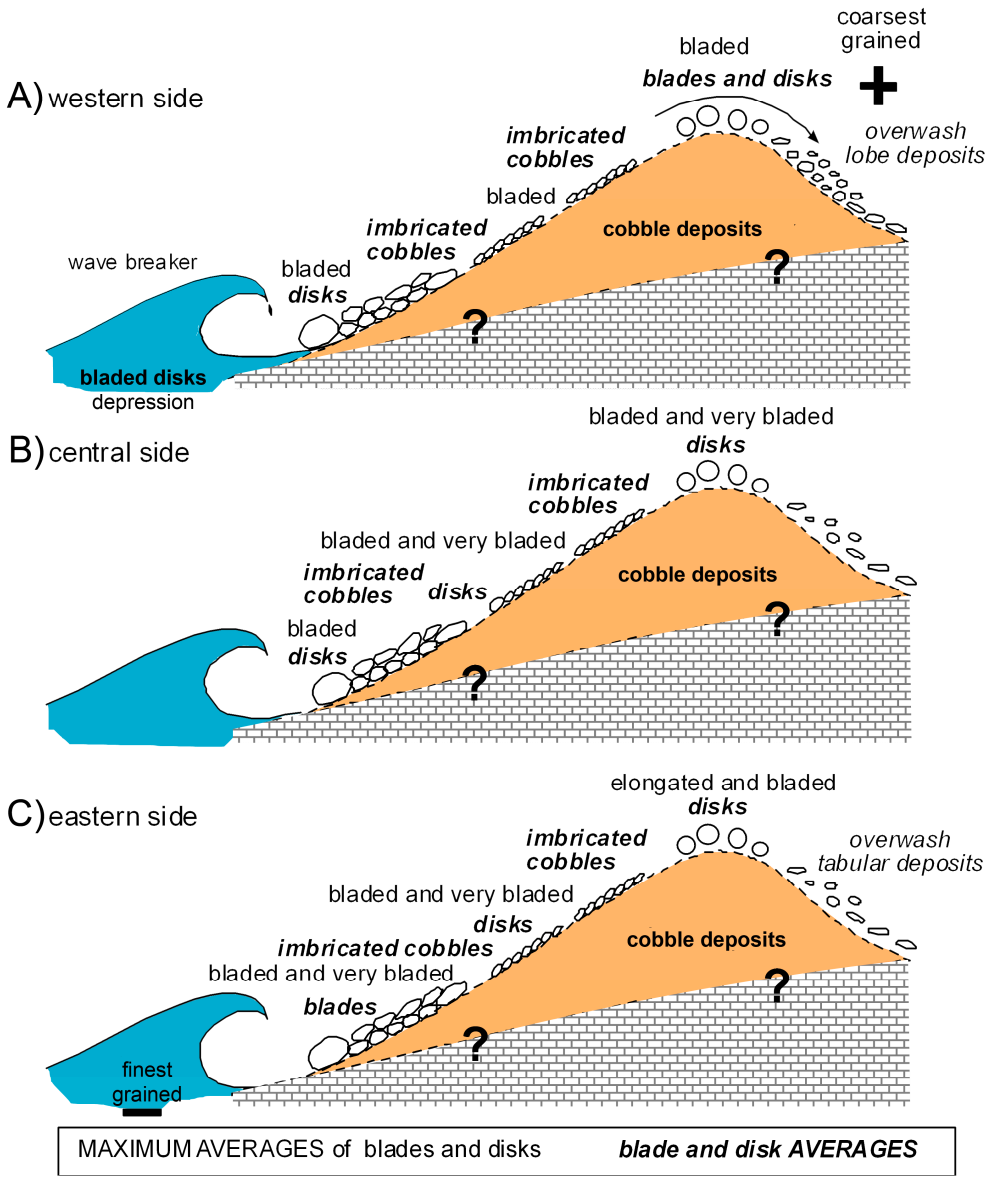

Figure 11. Synthesis of the cross-sectional distribution of cobble deposits from La Maruca/Pinquel beach according to particle shape in maximum percentages (normal) and averages (bold italics) for each station (without scale).

Particle morphology is an important characteristic of sediments, as this reflects their transport history and depositional environment [81].

The authors of [82] created an index of compactness calculated from the abovementioned morphological properties. Disks and spheroids usually show a tendency to be transported upslope, whereas spheres and rods mainly tend to be moved downslope. In the long term, particles tend to stabilize, so that disks and blades are located on the upper beach, while spheres and rods can be found downward [19].

In open sand beaches, grain size is coarser near the source and finer away from it [83]. At the local scale, especially in embayed beaches, grain size greatly varies spatially and temporarily [35]. Sediment sources and transport pathways are commonly inferred from grain-size data, and sorting is assumed to improve in the direction of transport [84,85] and in the lag deposit (McLaren model [86,87]). As sediments move downstream, their grain

size typically decreases and the shape of clasts becomes more rounded. Sorting improves as water separates particles by size, depositing larger particles closer to the source and smaller particles downstream. Sphericity increases as particles become more rounded, and angularity decreases as sharp edges and corners wear away [88].

Synthesis data for maximum and average percentages for each measurement station, in the present work, show that the dominant clast shape varies between disks and blades at the western culmination of the upper bar, with some differences in longitudinal direction (Figure 11A), whereas, on the rest of the beach, the dominant shape becomes disks (Figure 11B,C), followed by elongated forms [38]. In percentages, blade forms dominate but are replaced eastward by bladed and very bladed forms and, finally, elongated and bladed forms. In the intertidal band, disks and blades stabilized alternately without a clear tendency in the middle or intertidal foot or, even, in the elongated depression.

Even though certain differences can be observed both longitudinally and transversally (Figures 8 and 9) on the beach, generally more flattened forms are found in the upper part of the beach. This responds to the discoidal particles being more easily lodged in the upper part of the beach, despite its distance from the breakers, where most of the energy concentrates. This is possible given that pebbles show a better capacity for suspension and buoyancy [19]. Disks concentrate on the foreshore and elongated particles on the lower belt of the beach. The rod geometry of the latter allows them to roll more effectively down the foreshore, where swash and backwash processes represent the main dynamic process.

The morphosedimentary and dynamic model of La Maruca/Pinquel beach is relatively simple: incoming waves arrive obliquely in the direction NW–SE and are refracted regularly, without the beach rotating. Wave breaking occurs from approximately the mean rising tide in a homogeneous manner. In reflective beaches such as this, wave-energy dissipation by breaking is minimal [89]. The consensus in the literature is that, on gravel beaches, most sediment transport occurs in the swash zone rather than in the surf zone, causing the development of swash morphology [62]. However, this beach is characterized by the construction of berms and the arrangement of clasts exclusively by imbrication, i.e., the main transport of gravels presents transverse components: landward (more noticeable) and seaward (relatively stable).

On La Maruca/Pinquel beach, wave refraction manifests following a reorientation of the incoming waves, based on the recorded/deduced directionality (Figure 4B). This effect probably forces the incident waves to dissipate in a homogeneous manner along the foreshore.

During periods of calm, waves break over the cobble deposit and toward high tide on the rocky bottoms (wave-cut platform); the water column and the loose deposits placed in suspension are then directed both up the beach by back-and-forth processes and laterally as drift currents, mainly eastward.

Storm waves build tabular layers of pebbles and overwash lobes, comparable to fans on sandy beaches ("washover fans"). These usually show a greater development with spring high tides. From the cobble bar of this beach, which the author of [90] calls a solitary transgressive bar, with its upper berm toward low tide, the lower berms present shorter length and magnitude; both parameters stabilize toward the eastern edge following a clear stepping. The tidal zone allows for direct contact of the surface with the mass of seawater and the waves that play their erosive and sedimentary role on the beach, affecting a greater tidal range (macrotidal) or a lesser (microtidal) one.

The dominant size fraction (cobbles) presents high porosity, which determines the predominance of wave swash and swash infiltration in the foreshore [52]. Swash infiltration weakens the backwash, facilitating the persistence of imbrication in the foreshore [19,91].

The only relevant sedimentary structure on the study beach is represented by the upper slopes of 40° in the upper belt around the crest of the inner berm.

Longitudinal cobble transport is either minimal or non-existent (Figure 11B); however, granulometric parameters, mainly centile and mean grain size, decrease obliquely eastward and, partially, by sorting (Figure 8). This same eastward trend is deduced from the surface distribution of cobble shapes, particularly the roundness (Figure 9). This scenario can only be achieved during wave storms because calm periods are characterized by swash (more important) and backwash processes, a simple concave surface seaward, and the development of imbrication.

Along the foreshore, several staggered berms are built according to tidal ranges, and the ridges are remobilized to form overwash sheets and lobes (Figure 12A). This occurs throughout the entire foreshore, in both the upper and lower areas, representing a notable differential sign in this extended time period of 1984–2024 (Figure 10).

During prolonged calm periods, a shadow zone is stabilized in the western side, which tends to be colonized by fennel vegetation. However, the maximum sedimentation and covered area, which reached in the form of washover lobes, is replaced in the E by overwash tabular deposits (Figure 12B). Wave storms concentrate their greatest energy in this shadow area, generating or reactivating overwash lobes; as a result, landward migration is more significant (Figure 12B). This shadow zone contains a higher density of plant colonization. Within the exposed area of the eastern beach, the leeward zone of the large storm bar is a shadow area, with scarce, irregular, and dispersed plant colonization (Figure 12B). Paradoxically, the outer western shadow area coincides with environments that present the effects of storms, namely storm lobes.

Storm episodes are crucial in the distribution of gravel deposits since the predominating processes under these circumstances are those from the upper bar toward the backbeach (Figure 12A). Judging by the activation of overwash lobes in the western third of La Maruca/Pinquel beach (Figure 12B), wave storms are believed to enter this beach deviating according to an angle to the SW, probably over the channel-shaped depression, and to increase the water flow with a longitudinal component landward. These waves appear during each extraordinary stormy event, remobilizing the lower foreshore and stabilizing the cobbles that present the larger mean and centile size values (Table 2). Smaller storms build better tabular prisms, which cover a meter-wide belt, greater toward the center and the eastern corner of the beach.

Pure gravel beaches, such as the one analyzed in the present work, are highly reflective at all stages of the tidal cycle [92], and present a tide width that ranges from 18 to 50 m [80]. In La Maruca/Pinquel beach, grain size (centile and mean) decreases from W to E (Figure 8A,B); a cross-sectional trend is superimposed from coarse grain sizes at the storm upper berm decreasing to the lower swash foreshore (Figures 8B and 12A,B). Longitudinally, this same trend is reproduced, with larger sizes on the western side decreasing toward the eastern side (Figure 12B). Critical thresholds in sediment transport are commonly exceeded during wave storms, when mobility is high, resulting in a concentration of turbulent energy [79] capable of redistributing any grain fraction. Sediment grading along the beach commonly occurs due to the selective transport of finer clasts downstream of the unidirectional drift [65], for both sandy and gravel beaches.

The cobbles on the channel-shaped depression do not play any role in the dynamics of the study beach. The excess volume of the sedimentary prism is not significant; therefore, it does not favor the filling of this area. In addition, the presence of the green algal mat indicates the inactivity of these cobbles.

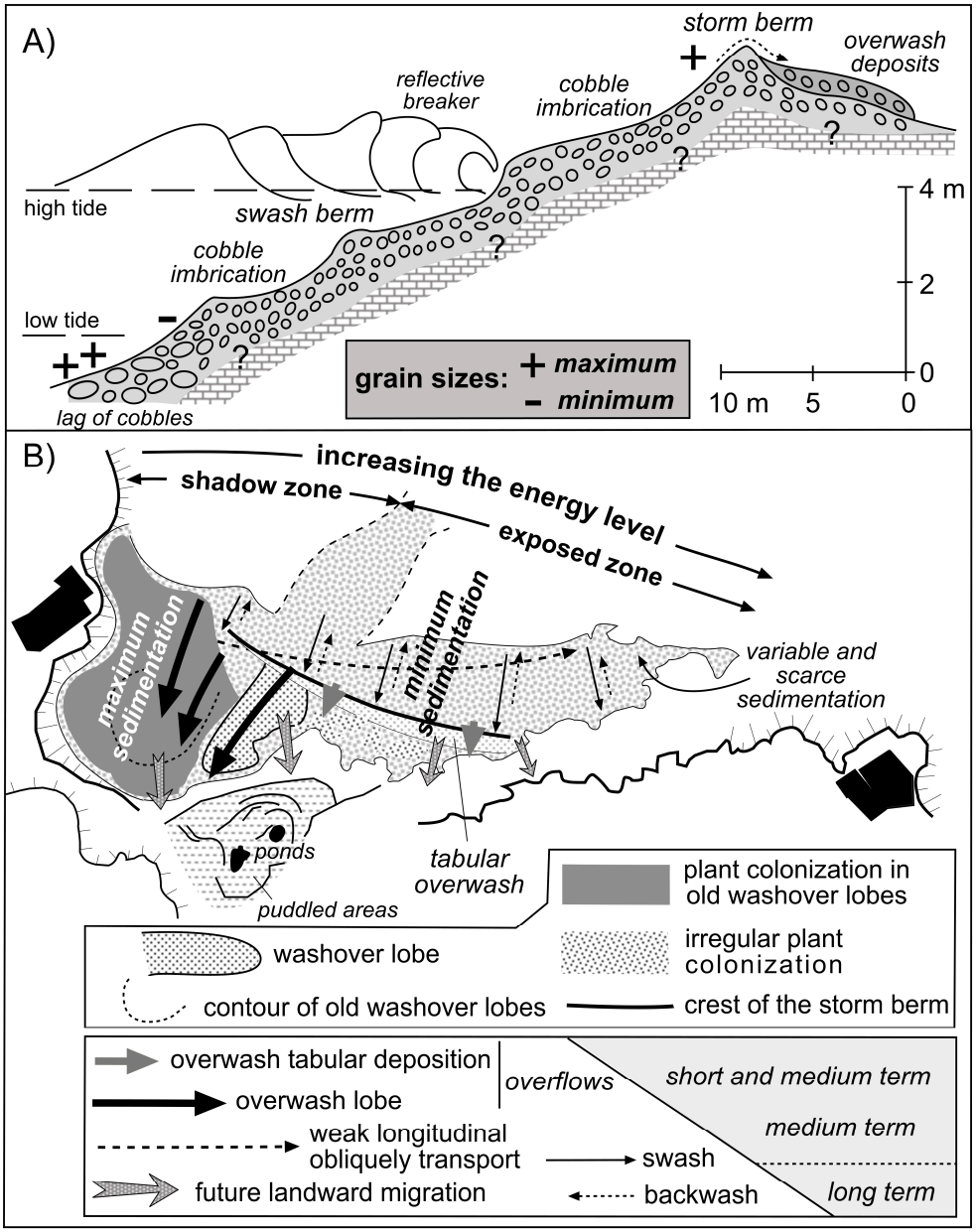

Figure 12. Pure reflective La Maruca/Pinquel cobble beach. (**A**) Diagram of the cross-sectional distribution, presenting morphologies and variation in mean grain sizes based partially on [80]. Lower belt represents the outer frame of [19]. (**B**) Morphosedimentary and dynamic model showing the stabilized crest of the storm bar/berm at the top of the beach, shaped and/or removed by storms, and the lower berms originated by back-and-forth processes. Overwash lobes are noticeable in the western area, where sedimentation is at its maximum; sediment volumes decrease eastward, where narrow overwash sheets are well represented.

6. Future Evolution Model

The flooding regime combining marine and meteorological dynamics in a specific stretch of coast is a complex phenomenon, as a large number of elements are involved. Sea-level changes are the result of the combined action of the mean sea level, the astronomical tide, and the meteorological residual [93]. The ongoing rise in sea level on a global scale plays a fundamental role, in the long term, in the migration of beaches, with a net component landward [46].

Waves in the Cantabrian Sea have significantly increased, at a rate of up to 0.8 cm/year for the most intense waves; by 2040, the trend of sea-level rise will mean average retreats

in beaches of about 3 m [56]. An increase in wave energy has concentrated on the high branch of the medium regime (H_{s12}), with waves increasing around 1.4 cm/year in the last 60 years [94], while the magnitude of the increase is lower for the extreme events (H_{T50}). These changes are causing a retreat of the coastline that can be early detected and that greatly impacts on the contact of beaches with their associated dune systems, such as the spits of Valdearenas, Somo, and La Salvé-Regatón, in Cantabria [95,96]. Cliff retreats have been documented in [97]. Their results show a significant increase in days with high sea levels, favorable to coastal erosion, during the last 50 years. However, this has been partially compensated by a reduction in the number of storms and a weakening of their average strength [98].

The advance of the sea inland involves a migration of the sedimentary prism by a typical retrogradation process within a generalized transgressive process. The author of [99] proposed pioneering responses of the behavior of the coastline to rising sea levels. The most widely used method to quantify the change in the coastline is the erosion rule, a generic and simple geometric model of evolution obtained from the cross-sectional profile of a beach in response to rising sea levels and assumed to be operational on all sandy coasts. Other models, such as the one in [100], introduce the estimated curve of sea-level rise until the year 2100. Other authors [101] use the response of the beach profile to sea-level change due only to the variation in transverse sediment transport. In the model proposed to show the response to sea-level rise (RD-A model in [102]), the profile is translated landward over a distance that is dependent on the average storm beach slope. Also, the authors of [103] described a simple model in a closed system where the beach sand volume is preserved and the beach profile shape is invariant. A modeling approach to shoreline evolution can predict short-term shoreline changes driven by waves and long-term changes driven by large-scale atmospheric patterns [104].

All the abovementioned models have been further detailed and broadened. The authors of [105] delved deeper into the issue, detailing the scope of application of the *Bruun rule* to coastal areas in the absence of other alternatives or data that would allow new modeling. In any case, they discourage its application in the future. In the case of [102], the author does not accept transfers of sandy masses to be identical in a longitudinal direction or dune fields to be ignored as an available sediment storage for the beach. His model includes beach–dune interaction and the consequent transverse transfer in both directions: landward with erosion and seaward with the incorporation of new embryonary aeolian dunes [106].

From the surfaces calculated in the orthophotos (Table 3) emerges a reduction in the area covered by clasts of 460.8 m^2 from 1984 (2.91×10^3 m^2) to 2024 (2.45×10^3 m^2), and probably an increase in vertical accumulation. Noticeable losses occurred during the strong storm surges of 2007–2008 and 2014 (2.44×10^3 m^2). Although irregularly, a significant decrease in surface took place in 2020, when the maximum surface did not of exceed 2.18×10^3 m^2, recovering to 2.45×10^3 m^2 in 2024 (Figure 13).

From the maps (Figure 10), the retreats of the upper berm crest were calculated for the period from 1984 to 2024 at about 12 m (Figure 13). Intervals with high retreat rates, increasing from 1984 to 2010 (0.19 m/year to 0.92 m/year), and intervals of inactivity from 2010 to 2017 were identified, with the latter paradoxically coinciding with strong storms in the winters of 2008–2009 [78] and 2014 [75,76,107]. During the periods 2017 to 2020 and 2020 to 2024, the rates were estimated at 0.27 and 0.62 m/year, respectively. A mean retreat rate of 0.042 m/year was calculated for the Cantabrian cliffs [49], a much lower rate than that experienced by the Maruca deposits. A similar future behavior of this central and eastern beach can be expected as well as a landward migration in the same direction of the overwash lobes in the western one.

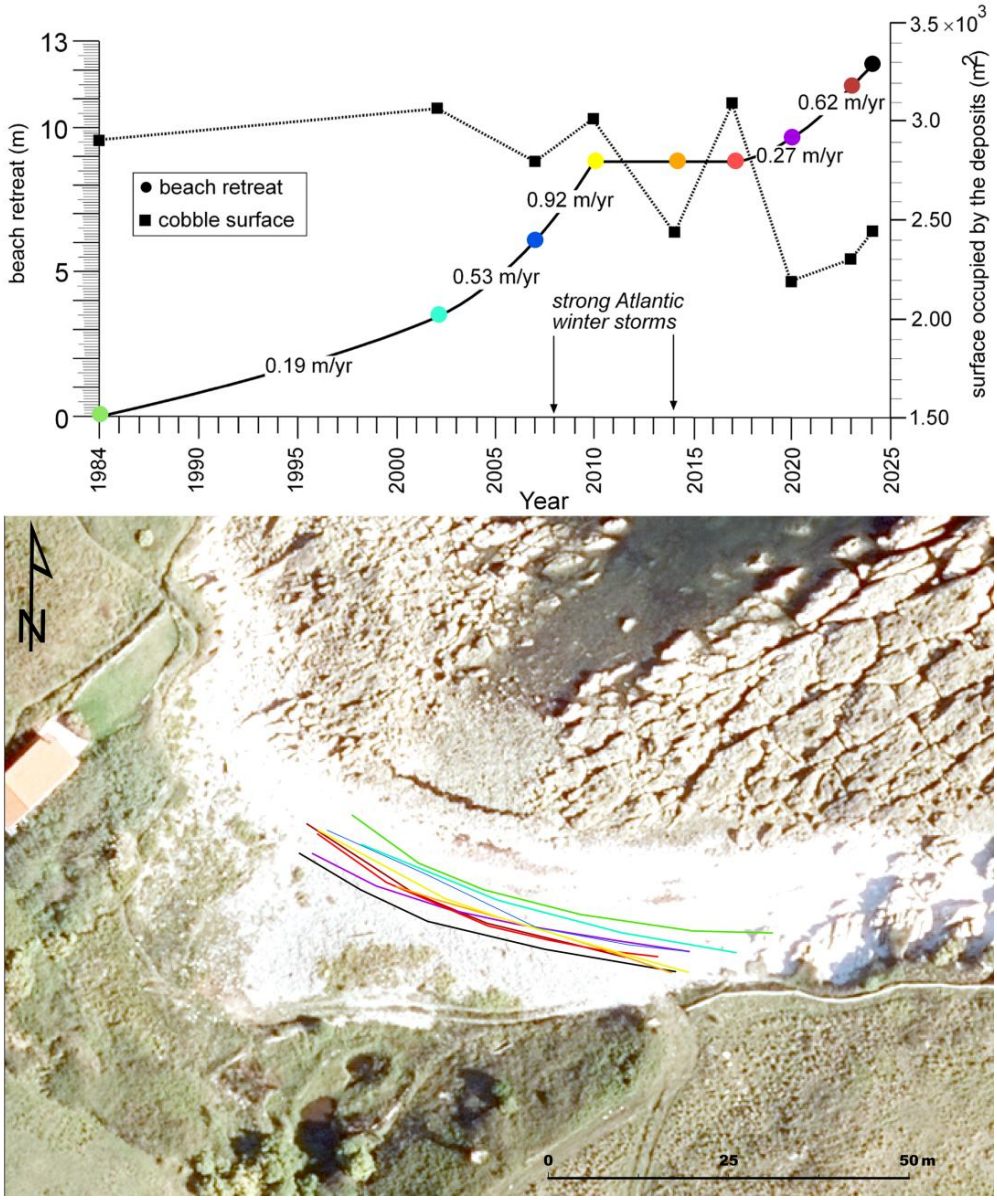

Figure 13. Beach retreat from 1984 to 2024, in different colors, based on the landward migration of the storm crest of the upper berm (meters), and the rise rates for each interval. The surfaces occupied by cobbles are calculated for the same period. The left vertical axis represents the horizontal retreat (in m) or migration of beach deposits, while the right vertical axis shows the area occupied in each record. The calculated retreat rate (m/year) is obtained from two successive records (Table 3).

The inner belt of the wave-cut platform in contact with the foreshore foot has been intensely worn away (Figure 6F,G), mostly on the eastern beach, explaining the changes in the surface area of the subsequently ejected cobbles.

The presence of a relative wide and flat backbeach at La Maruca/Pinquel, with karstic ponds and puddles (Figure 12B), as a potential receiving area for migrating landward beach sediments, will facilitate the future settlement of the beach cobble prism, maintaining a similar geometry and keeping the granulometries, shapes of the clasts, and volumes of deposit unchanged. The presence of the wave-cut platform in the lower intertidal zone, elevated with respect to the current sedimentary foot, could guarantee the future stability of the beach against sea-level rise by dissipating the energy of breaking waves.

7. Conclusions

This study focuses its attention on the analysis of the morphology of a cobble beach composed of a dynamic upper ridge and several ephemeral tidal berms (up to three).

Granulometric data and cobble shape analyses were applied to assess the beach's morphodynamic state, which corresponds to summer conditions characterized by calm wave activity. Most cobble deposits exhibit widespread imbrication structures. Trend maps of these sedimentological parameters, combined with detailed beach cartography, proved to be highly effective tools in the identification of spatial variations and the sediment transport pathways inferred from them.

From the upper crest to the lower intertidal zone and eastward areas, grain size decreases obliquely, reflecting a weak longshore drift. The initially poor sorting observed in the upper western sector shows improvement due to an eastward sediment transport trend.

An increase in mean grain size is associated with enhanced particle roundness, while other correlation indices show a declining trend. The dominant clast shapes are disks and blades, with average roundness values reaching medium–high levels (0.63). No consistent spatial trends in clast shape are observed across the beach surface.

Morphological changes over the past 40 years (1984–2024) were documented in this work, highlighting the relative persistence of the upper berm (beach ridge), along with variable tidal berms, washovers, sheets, and depositional lobes. These features enabled the projection of future morphological evolution.

During this period, the beach has migrated landward by approximately 12 m, accompanied by a reduction of around 460.8 m^2 in the area covered by cobble deposits. This loss has been partially offset by an increase in ridge height and landward migration, primarily driven by overwash lobe development. The cobble ridge and intertidal zone are expected to continue migrating landward, accompanied by the formation of new tidal berms and overwash lobes.

As the retreat trend accelerates exponentially, the rate of shoreline retreat is projected to increase in the coming years. For this reason, whoever might be responsible for its management should pay close attention to future changes, as these may serve as indicators of the beach's stability.

Author Contributions: G.F. conceived the idea of the work and the methodology. J.B. implemented the methodological development and supervised the findings of this work. G.F. wrote the original draft. J.B. and G.F. reviewed and edited the final work. All authors discussed the results and contributed to the final manuscript. All authors have read and agreed to the published version of the manuscript.

Funding: This research was funded by "Caracterización de materiales, formas y procesos recientes para mejorar la gestión de los recursos y riesgos geológicos" (29.P209.64004, Universidad de Cantabria).

Data Availability Statement: The new data presented in this study are available from the corresponding author upon request.

Acknowledgments: The authors thank the anonymous reviewers, whose comments improved this paper significantly.

Conflicts of Interest: The authors declare no conflicts of interest.

References

1. Silva, R.; Martínez, M.L.; Van Tussenbroek, B.I.; Guzmán-Rodríguez, L.O.; Mendoza, E.; López-Portillo, J. A Framework to Manage Coastal Squeeze. *Sustainability* **2020**, *12*, 10610. [CrossRef]
2. Usai, A.; Simeone, S.; Trogu, D.; Porta, M.; De Muro, S. A Morphometric Analysis of Embayed Beaches: Southern Sardinia Island. *Geomorphology* **2025**, *483*, 109838. [CrossRef]

3. Dalezios, N.R.; Eslamian, S.; Ostad-Ali-Askari, K.; Rabbani, S.; Saeidi-Rizi, A. Sediments. In *Encyclopedia of Engineering Geology*; Bobrowsky, P.T., Marker, B., Eds.; Encyclopedia of Earth Sciences Series; Springer International Publishing: Cham, Switzerland, 2018; pp. 818–819. ISBN 978-3-319-73566-5.
4. Folk, R.L.; Ward, W.C. Brazos River Bar [Texas]; a Study in the Significance of Grain Size Parameters. *J. Sediment. Res.* **1957**, *27*, 3–26. [CrossRef]
5. Bujan, N.; Cox, R.; Masselink, G. From Fine Sand to Boulders: Examining the Relationship between Beach-Face Slope and Sediment Size. *Mar. Geol.* **2019**, *417*, 106012. [CrossRef]
6. Barrett, P.J. The Shape of Rock Particles, a Critical Review. *Sedimentology* **1980**, *27*, 291–303. [CrossRef]
7. Grottoli, E.; Bertoni, D.; Ciavola, P. Short-and Medium-Term Response to Storms on Three Mediterranean Coarse-Grained Beaches. *Geomorphology* **2017**, *295*, 738–748. [CrossRef]
8. Wright, L.D.; Short, A.D. Morphodynamic Variability of Surf Zones and Beaches: A Synthesis. *Mar. Geol.* **1984**, *56*, 93–118. [CrossRef]
9. Masselink, G.; Short, A.D. The Effect of Tide Range on Beach Morphodynamics and Morphology: A Conceptual Beach Model. *J.Coast. Res.* **1993**, *9*, 785–800. Available online: https://www.jstor.org/stable/4298129 (accessed on 20 October 2025).
10. Buscombe, D.; Masselink, G. Concepts in Gravel Beach Dynamics. *Earth-Sci. Rev.* **2006**, *79*, 33–52. [CrossRef]
11. Etienne, S.; Paris, R. Boulder Accumulations Related to Storms on the South Coast of the Reykjanes Peninsula (Iceland). *Geomorphology* **2010**, *114*, 55–70. [CrossRef]
12. Costa, S.; Levoy, F.; Monfort, O.; Curoy, J.; De Saint Léger, E.; Delahaye, D. Impact of Sand Content and Cross-Shore Transport on the Morphodynamics of Macrotidalgravel Beaches (Haute-Normandie, English Channel). *Z. Geomorphol.* **2008**, *52*, 41–62. [CrossRef]
13. Lorang, M.S. Predicting Threshold Entrainment Mass for a Boulder Beach. *J. Coast. Res.* **2000**, *16*, 432–445.
14. Soloy, A.; Lopez Solano, C.; Turki, E.I.; Mendoza, E.T.; Lecoq, N. Rapid Changes in Permeability: Numerical Investigation into Storm-Driven Pebble Beach Morphodynamics with XBeach-G. *J. Mar. Sci. Eng.* **2024**, *12*, 327. [CrossRef]
15. Nielsen, P.; Hanslow, D.J. Wave Runup Distributions on Natural Beaches. *J. Coast. Res.* **1991**, *7*, 1139–1152.
16. Bujak, D.; Ilic, S.; Miličević, H.; Carević, D. Wave Runup Prediction and Alongshore Variability on a Pocket Gravel Beach under Fetch-Limited Wave Conditions. *J. Mar. Sci. Eng.* **2023**, *11*, 614. [CrossRef]
17. Polidoro, A. The Effect of Grain Size Distribution and Bimodal Sea States on Coarse Beach Sediment Dynamics. Ph.D. Thesis, The Open University, Milton Keynes, UK, 2018.
18. Martos de la Torre, E. Evolución Morfosedimentaria de La Playa de Cantos de Aramar. Master's Thesis, University of Oviedo, Oviedo, Spain, 2003.
19. Bluck, B.J. Sedimentation of Beach Gravels; Examples from South Wales. *J. Sediment. Res.* **1967**, *37*, 128–156. [CrossRef]
20. Fellowes, T.E.; Vila-Concejo, A.; Gallop, S.L. Morphometric Classification of Swell-Dominated Embayed Beaches. *Mar. Geol.* **2019**, *411*, 78–87. [CrossRef]
21. Sutherland, R.A.; Lee, C.T. Discrimination between Coastal Subenvironments using Textural Characteristics. *Sedimentology* **1994**, *41*, 1133–1145. [CrossRef]
22. Hampton, M.A.; Griggs, G.B.; Edil, T.B.; Guy, D.E.; Kelley, J.T.; Komar, P.D.; Mickelston, D.M.; Shipman, H.M. Formation, Evolution, and Stability of Coastal Cliffs–Status and Trends. In *U.S. Geological Survey Professional Paper 1693*; United States Geological Survey: Reston, VA, USA, 1984; pp. 1–4.
23. Bonachea, J.; Remondo, J.; Rivas, V. Estuaries in Northern Spain: An Analysis of Their Sedimentation Rates. *Sustainability* **2024**, *16*, 6856. [CrossRef]
24. Barnolas, A.; Pujalte, V. La Cordillera Pirenaica: Definición, Límites y División. In *Geología de España*; Vera, J.A., Ed.; IGME: Madrid, Spain, 2004; pp. 233–241.
25. Ramírez del Pozo, J.; Portero García, J.M. *Mapa Geológico de España, Escala 1:50,000. Hoja Geológica de Santander 35*; IGME: Madrid, Spain, 1976.
26. García-Herrera, G. Estudio Geológico-Geotécnico del Subsuelo Urbano de la Ciudad de Santander. Master's Thesis, University of Oviedo, Oviedo, Spain, 2013.
27. Google Earth. Available online: https://earth.google.com (accessed on 5 August 2025).
28. Mapas Cantabria. Visualizador de Mapas del Gobierno de Cantabria. Available online: https://mapas.cantabria.es (accessed on 5 August 2025).
29. Instituto Geográfico Nacional. Centro de Descargas Del CNIG (IGN). Available online: https://centrodedescargas.cnig.es/CentroDescargas/ortofoto-pnoa-maxima-actualidad (accessed on 5 August 2025).
30. Instituto Geográfico Nacional. Plan Nacional de Ortofotografía Aérea. Available online: https://pnoa.ign.es/web/portal/pnoa-imagen/ortofotos-pnoa-anuales (accessed on 5 August 2025).
31. Tutiempo Network, S.L. Tabla de Mareas en Santander marzo de 2023 (Cantabria). Available online: https://www.tutiempo.net/mareas/espana/santander/marzo-2023.html (accessed on 5 August 2025).

32. Emery, K.O. A Simple Method of Measuring Beach Profiles. *Limnol. Oceanogr.* **1961**, *6*, 90–93. [CrossRef]
33. Delgado, I.; Lloyd, G. A Simple Low-Cost Method for One Person Beach Profiling. *J. Coast. Res.* **2004**, *204*, 1246–1252. [CrossRef]
34. Chowdhury, S.R.; Hossain, M.S.; Sharifuzzaman, S.M. A Simple and Inexpensive Method for Muddy Shore Profiling. *Chin. J. Ocean. Limnol.* **2014**, *32*, 1383–1391. [CrossRef]
35. Prodger, S.; Russell, P.; Davidson, M. Grain-Size Distributions on High-Energy Sandy Beaches and their Relation to Wave Dissipation. *Sedimentology* **2017**, *64*, 1289–1302. [CrossRef]
36. Orford, J.D. Discrimination of Particle Zonation on a Pebble Beach. *Sedimentology* **1975**, *22*, 441–463. [CrossRef]
37. Switzer, A.D. 14.19 Measuring and Analyzing Particle Size in a Geomorphic Context. In *Treatise on Geomorphology*; Elsevier: Amsterdam, The Netherlands, 2013; pp. 224–242. ISBN 978-0-08-088522-3.
38. Dobkins, J.E.; Folk, R.L. Shape Development on Tahiti-Nui. *J. Sediment. Res.* **1970**, *40*, 1167–1203. [CrossRef]
39. Blott, S.J.; Pye, K. Gradistat: A Grain Size Distribution and Statistics Package for the Analysis of Unconsolidated Sediments. *Earth Surf. Process. Landf.* **2001**, *26*, 1237–1248. [CrossRef]
40. Flor, G.; Martínez Cedrún, P. Saucer Blowouts in the Coast Dune Fields of NW Spain. *J. Iber. Geol.* **2024**, *50*, 227–248. [CrossRef]
41. Oakey, R.J.; Green, M.; Carling, P.A.; Lee, M.W.E.; Sear, D.A.; Warburton, J. Grain-Shape Analysis-A New Method for Determining Representative Particle Shapes for Populations of Natural Grains. *J. Sediment. Res.* **2005**, *75*, 1065–1073. [CrossRef]
42. Folk, R.L. Student Operator Error in Determination of Roundness, Sphericity, and Grain Size. *J. Sediment. Res.* **1955**, *25*, 297–301. [CrossRef]
43. Karditsa, A.; Poulos, S.E. The Application of Grain Size Trend Analysis in the Fine Grained Seabed Sediment of Alexandroupolis Gulf. *Bull. Geol. Soc. Greece* **2016**, *47*, 157. [CrossRef]
44. Poizot, E.; Méar, Y.; Biscara, L. Sediment Trend Analysis through the Variation of Granulometric Parameters: A Review of Theories and Applications. *Earth-Sci. Rev.* **2008**, *86*, 15–41. [CrossRef]
45. Dickson, M.E.; Kench, P.S.; Kantor, M.S. Longshore Transport of Cobbles on a Mixed Sand and Gravel Beach, Southern Hawke Bay, New Zealand. *Mar. Geol.* **2011**, *287*, 31–42. [CrossRef]
46. Orford, J.D.; Carter, R.W.G.; Forbes, D.L. Gravel Barrier Migration and Sea Level Rise: Some Observations from Story Head, Nova Scotia, Canada. *J. Coast. Res.* **1991**, *7*, 477–489. Available online: http://www.jstor.org/stable/4297854 (accessed on 20 October 2025).
47. Erikson, L.H.; O'Neill, A.C.; Barnard, P.L.; Vitousek, S.; Limber, P.W. Climate Change-Driven Cliff and Beach Evolution at Decadal to Centennial Time Scales. In Proceedings of the Proceedings Coastal Dynamics 2017, Helsingør, Denmark, 12–16 June 2017; pp. 125–136.
48. Puertos del Estado: PORTUS. Available online: https://portus.puertos.es (accessed on 5 August 2025).
49. Rueda, A.; Costales, A.; Bruschi, V.; Sánchez-Espeso, J.; Méndez, F. Regional Coastal Cliff Classification: Application to the Cantabrian Coast, Spain. *Estuar. Coast. Shelf Sci.* **2024**, *308*, 108900. [CrossRef]
50. Tomasicchio, G.R.; Archetti, R.; D'Alessandro, F.; Sloth, P. Long Shore Transport at Berm Breakwaters and Gravel Beaches. In Coastal Structures 2007, Proceedings of the 5th Coastal Structures International Conference, CSt07, Venice, Italy, 2–4 July 2007; World Scientific Publishing Company: Venice, Italy, 2009; pp. 65–76.
51. Flor, G.; Flor-Blanco, G. Aspectos Morfológicos, Dinámicos y Sedimentarios del Sector Costero: Desembocadura del Nalón-Playa de Bañugues: Problemática Ambiental. In *Guía de Campo*; University of Oviedo: Oviedo, Spain, 2009.
52. Dashtgard, S.E.; MacEachern, J.A.; Frey, S.E.; Gingras, M.K. Tidal Effects on the Shoreface: Towards a Conceptual Framework. *Sediment. Geol.* **2012**, *279*, 42–61. [CrossRef]
53. Short, A.D.; Masselink, G. Embayed and Structurally Controlled Beaches. In *Handbook of Beach and Shoreface Morphodynamics*; Short, A.D., Ed.; John Wiley and Sons Ltd.: Hoboken, NJ, USA, 1999; pp. 230–250. ISBN 978-0-471-96570-1.
54. Chust, G.; González, M.; Fontán, A.; Revilla, M.; Alvarez, P.; Santos, M.; Cotano, U.; Chifflet, M.; Borja, A.; Muxika, I.; et al. Climate Regime Shifts and Biodiversity Redistribution in the Bay of Biscay. *Sci. Total Environ.* **2022**, *803*, 149622. [CrossRef]
55. Medina, R.; Méndez, F.J. Inundación Costera Originada por la Dinámica Marina. *Ingeniería y Territorio* **2006**, *74*, 68–75.
56. Losada, I.; Izaguirre, C.; Diaz, P. *Cambio Climático En La Costa Española*; Oficina Española de Cambio Climático, Ministerio de Agricultura, Alimentación y Medio Ambiente: Madrid, Spain, 2014; p. 133.
57. Hoyos, S.; González, A.; Díaz de Terán, J.R. Geología y Geomorfología de La Península de La Magdalena. In *Estudio del Medio Físico. Plan Director de la Península de la Magdalena*; Sáinz Vidal, E., Ed.; Ayuntamiento de Santander: Santander, UK, 2008; pp. 43–53.
58. Larson, M.; Donnelly, C.; Jiménez, J.A.; Hanson, H. Analytical Model of Beach Erosion and Overwash during Storms. *Proc. Inst. Civ. Eng.-Marit. Eng.* **2009**, *162*, 115–125. [CrossRef]
59. Hayes, M.O.; Michel, J.; Betenbaugh, D.V. The Intermittently Exposed, Coarse-Grained Gravel Beaches of Prince William Sound, Alaska: Comparison with Open-Ocean Gravel Beaches. *J. Coast. Res.* **2010**, *2010*, 4–30. [CrossRef]
60. Masselink, G.; Li, L. The Role of Swash Infiltration in Determining the Beachface Gradient: A Numerical Study. *Mar. Geol.* **2001**, *176*, 139–156. [CrossRef]

61. Weir, F.M.; Hughes, M.G.; Baldock, T.E. Beach Face and Berm Morphodynamics Fronting a Coastal Lagoon. *Geomorphology* **2006**, *82*, 331–346. [CrossRef]
62. Poate, T.; Masselink, G.; Davidson, M.; McCall, R.; Russell, P.; Turner, I. High Frequency In-Situ Field Measurements of Morphological Response on a Fine Gravel Beach during Energetic Wave Conditions. *Mar. Geol.* **2013**, *342*, 1–13. [CrossRef]
63. Komar, P.D. *Beach Processes and Sedimentation*, 2nd ed.; Prentice Hall: Lebanon, IN, USA, 1998; Volume 1, ISBN 978-0-13-754938-2.
64. Bryant, E. Behavior of Grain Size Characteristics on Reflective and Dissipative Foreshores, Broken Bay, Australia. *J. Sediment. Res.* **1982**, *52*, 431–450. [CrossRef]
65. Anthony, E.J. Chapter Six Gravel Beaches and Barriers. *Dev. Mar. Geol.* **2008**, *4*, 289–324. [CrossRef]
66. Kirk, R.M. Mixed Sand and Gravel Beaches: Morphology, Processes and Sediments. *Prog. Phys. Geogr. Earth Environ.* **1980**, *4*, 189–210. [CrossRef]
67. Roberts, T.M.; Wang, P.; Puleo, J.A. Storm-Driven Cyclic Beach Morphodynamics of a Mixed Sand and Gravel Beach along the Mid-Atlantic Coast, USA. *Mar. Geol.* **2013**, *346*, 403–421. [CrossRef]
68. Loureiro, C.; Ferreira, Ó. Mechanisms and Timescales of Beach Rotation. In *Sandy Beach Morphodynamics*; Elsevier: Amsterdam, The Netherlands, 2020; pp. 593–614. [CrossRef]
69. Wang, J.; You, Z.J.; Liang, B. Laboratory Investigation of Coastal Beach Erosion Processes under Storm Waves of Slowly Varying Height. *Mar. Geol.* **2020**, *430*, 106321. [CrossRef]
70. Bascom, W.N. The Relationship between Sand Size and Beach-Face Slope. *Eos Trans. Am. Geophys. Union* **1951**, *32*, 866–874. [CrossRef]
71. McFall, B.C. The Relationship between Beach Grain Size and Intertidal Beach Face Slope. *J. Coast. Res.* **2019**, *35*, 1080–1086. [CrossRef]
72. McLean, R.F.; Kirk, R.M. Relationships between Grain Size, Size-Sorting, and Foreshore Slope on Mixed Sand-Shingle Beaches. *N. Z. J. Geol. Geophys.* **1969**, *12*, 138–155. [CrossRef]
73. Ortega-Sánchez, M.; Fachin, S.; Sancho, F.; Losada, M.A. Relation between Beachface Morphology and Wave Climate at Trafalgar Beach (Cádiz, Spain). *Geomorphology* **2008**, *99*, 171–185. [CrossRef]
74. Castelle, B.; Marieu, V.; Bujan, S.; Splinter, K.D.; Robinet, A.; Sénéchal, N.; Ferreira, S. Impact of the Winter 2013–2014 Series of Severe Western Europe Storms on a Double-Barred Sandy Coast: Beach and Dune Erosion and Megacusp Embayments. *Geomorphology* **2015**, *238*, 135–148. [CrossRef]
75. Masselink, G.; Castelle, B.; Scott, T.; Dodet, G.; Suanez, S.; Jackson, D.; Floc'h, F. Extreme Wave Activity during 2013/2014 Winter and Morphological Impacts along the Atlantic Coast of Europe. *Geophys. Res. Lett.* **2016**, *43*, 2135–2143. [CrossRef]
76. Flor, G.; Flor-Blanco, G.; Flores, C. Cambios Ambientales por los Temporales de Invierno de 2014 en la Costa Asturiana (NO de España). *Trab. De Geol.* **2014**, 97–123. [CrossRef]
77. Manero-Lecea, G. Análisis de los Temporales Marinos entre 2013–2014 y de sus Impactos en las Costas de Cantabria. Master's Thesis, University of Cantabria, Santander, Spain, 2015.
78. Garrote, J.; Díaz-Álvarez, A.; Nganhane, H.V.; Heydt, G.G. The Severe 2013–14 Winter Storms in the Historical Evolution of Cantabrian (Northern Spain) Beach-Dune Systems. *Geosciences* **2018**, *8*, 459. [CrossRef]
79. Austin, M.J.; Buscombe, D. Morphological Change and Sediment Dynamics of the Beach Step on a Macrotidal Gravel Beach. *Mar. Geol.* **2008**, *249*, 167–183. [CrossRef]
80. Jennings, R.; Shulmeister, J. A Field Based Classification Scheme for Gravel Beaches. *Mar. Geol.* **2002**, *186*, 211–228. [CrossRef]
81. Pettijohn, F.J.; Potter, P.E.; Siever, R. *Sand and Sandstone*; Springer: New York, NY, USA, 1973; ISBN 978-0-387-90071-1.
82. Angelidakis, V.; Nadimi, S.; Utili, S. Elongation, Flatness and Compactness Indices to Characterise Particle Form. *Powder Technol.* **2022**, *396*, 689–695. [CrossRef]
83. Huisman, B.J.A.; de Schipper, M.A.; Ruessink, B.G. Sediment Sorting at the Sand Motor at Storm and Annual Time Scales. *Mar. Geol.* **2016**, *381*, 209–226. [CrossRef]
84. Inman, D.L. Sorting of Sediments in the Light of Fluid Mechanics. *J. Sediment. Res.* **1949**, *19*, 51–70. [CrossRef]
85. Folk, R.L. A Review of Grain-Size Parameters. *Sedimentology* **1966**, *6*, 73–93. [CrossRef]
86. McLaren, P. An Interpretation of Trends in Grain-Size Measures. *J. Sediment. Res.* **1981**, *51*, 611–624. [CrossRef]
87. McLaren, P.; Bowles, D. The Effects of Sediment Transport on Grain-Size Distributions. *J. Sediment. Res.* **1985**, *55*, 457–470. [CrossRef]
88. Marshak, S. *Earth: Portrait of a Planet/Stephen Marshak*; W. W. Norton and Company: New York, NY, USA, 2019; ISBN 978-0-393-64031-1.
89. Sherman, D.J. Reflective Beaches. In *Encyclopedia of Coastal Science*; Schwartz, M.L., Ed.; Springer: Dordrecht, The Netherlands, 2005; pp. 795–797. ISBN 978-1-4020-3880-8.
90. Carter, R.W. *Coastal Environments*; Academic Press: Cambridge, MA, USA; Elsevier: London, UK, 1988; ISBN 978-0-08-050214-4.
91. Tanner, L.H. Gravel Imbrication on the Deflating Backshores of Beaches on Prince Edward Island, Canada. *Sediment. Geol.* **1996**, *101*, 145–148. [CrossRef]

92. Carter, R.W.G.; Orford, J.D. The Morphodynamics of Coarse Clastic Beaches and Barriers: A Short- and Long-Term Perspective. *J. Coast. Res. 1993*, 158–179. Available online: http://www.jstor.org/stable/25735728 (accessed on 20 October 2025).
93. Menéndez-García, M.; Pérez-García, J.; Méndez-Incera, F.J.; Izaguirre-Lasa, C. Arcimis: Cambios en los Eventos Extremos de Inundación en la Costa. In *Publicaciones de la Asociación Española de Climatología. Serie A*; Asociación Española de Climatología: Madrid, Spain, 2012.
94. Losada, I.; Toimil-Silva, A.; Díaz-Simal, P. *Asistencia Técnica a La Elaboración de Un Estudio Sobre La Adaptación al Cambio Climático de La Costa Del Principado de Asturias. Actividad 3: Estrategia de Adaptación*; Ministerio de Agricultura, Alimentación y Medio Ambiente: Madrid, Spain, 2015; pp. 1–312.
95. De Sanjosé Blasco, J.J.; Gómez-Lende, M.; Sánchez-Fernández, M.; Serrano-Cañadas, E. Monitoring Retreat of Coastal Sandy Systems Using Geomatics Techniques: Somo Beach (Cantabrian Coast, Spain, 1875–2017). *Remote Sens.* **2018**, *10*, 1500. [CrossRef]
96. Flor, G.; Flor-Blanco, G.; Martínez-Cedrún, P.; Flores-Soriano, C.; Borghero, C. Aeolian Dune Fields in the Coasts of Asturias and Cantabria (Spain, NW Iberian Peninsula). In *The Spanish Coastal Systems: Dynamic Processes, Sediments and Management*; Morales, J.A., Ed.; Springer International Publishing: Cham, Switzerland, 2019; pp. 585–609. ISBN 978-3-319-93169-2.
97. De Sanjosé Blasco, J.J.; Serrano-Cañadas, E.; Sánchez-Fernández, M.; Gómez-Lende, M.; Redweik, P. Application of Multiple Geomatic Techniques for Coastline Retreat Analysis: The Case of Gerra Beach (Cantabrian Coast, Spain). *Remote Sens.* **2020**, *12*, 3669. [CrossRef]
98. García-Codrón, J.C.; Rasilla-Álvarez, D.F. Coastline Retreat, Sea Level Variability and Atmospheric Circulation in Cantabria (Northern Spain). *J. Coast. Res. 2006*, 49–54. Available online: http://www.jstor.org/stable/25737381 (accessed on 20 October 2025).
99. Bruun, P. Sea-Level Rise as a Cause of Shore Erosion. *J. Waterw. Harb. Div.* **1962**, *88*, 117–130. [CrossRef]
100. Dean, R.G. Additional Sediment Transport Input to Nearshore Region. *Shore Beach* **1987**, *55*, 76–81.
101. Kriebel, D.L.; Dean, R.G. Convolution Method for Time-Dependent Beach-Profile Response. *J. Waterw. Port Coast. Ocean. Eng.* **1993**, *119*, 204–226. [CrossRef]
102. Davidson-Arnott, R.G.D. Conceptual Model of the Effects of Sea Level Rise on Sandy Coasts. *J. Coast. Res.* **2005**, *21*, 1166–1172. [CrossRef]
103. Taborda, R.; Ribeiro, M.A. A Simple Model to Estimate the Impact of Sea-Level Rise on Platform Beaches. *Geomorphology* **2015**, *234*, 204–210. [CrossRef]
104. Montaño, J.; Coco, G.; Cagigal, L.; Mendez, F.; Rueda, A.; Bryan, K.R.; Harley, M.D. A Multiscale Approach to Shoreline Prediction. *Geophys. Res. Lett.* **2021**, *48*, e2020GL090587. [CrossRef]
105. Cooper, J.A.G.; Pilkey, O.H. Sea-Level Rise and Shoreline Retreat: Time to Abandon the Bruun Rule. *Glob. Planet. Change* **2004**, *43*, 157–171. [CrossRef]
106. Flor-Blanco, G.; Flor, G.; Pando, L. Evolution of the Salinas-El Espartal and Xagó Beach/Dune Systems in North-Western Spain over Recent Decades: Evidence for Responses to Natural Processes and Anthropogenic Interventions. *Geo-Mar. Lett.* **2013**, *33*, 143–157. [CrossRef]
107. Rasilla, D.; García-Codron, J.C.; Garmendia, C.; Herrera, S.; Rivas, V. Extreme Wave Storms and Atmospheric Variability at the Spanish Coast of the Bay of Biscay. *Atmosphere* **2018**, *9*, 316. [CrossRef]